ELSEVIER

Coordination Chemistry Reviews
156 (1996) 275–332

COORDINATION CHEMISTRY REVIEWS

Structural aspects of Pt complexes containing model nucleobases

Ennio Zangrando [a], Fabio Pichierri [a], Lucio Randaccio [a], Bernhard Lippert [b]

[a] *Dipartimento di Scienze Chimiche, Università di Trieste, I-34127 Trieste, Italy*
[b] *Fachbereich Chemie, Universität Dortmund, D-44221 Dortmund, Germany*

Received 2 August 1995; accepted 15 September 1995

Contents

SSDI 0010-8545(95)01250-X

Abstract

Compounds of Pt(II) and Pt(IV)-containing nucleobases as ligands (also including a few related ligands) are summarized and described, according to the nuclearity of the complexes. The large amount of available crystallographic data allows geometrical parameters such as bond lengths and angles, angular distortions, torsional angles related to the nucleobase plane orientations etc., to be derived with relatively high accuracy. Simple relationships between some of these parameters are reported and discussed. On mononuclear Pt complexes containing one or more nucleobase ligands a simple descriptive statistical analysis has been performed. The structural properties of polynuclear, often heteronuclear species have also been reviewed, where the nucleobases, particularly pyrimidines, act as polydentate–often bridging–ligands. A simple MO theoretical analysis of the metal–metal interaction in homo- and heterodinuclear species allows the degree of the intermetallic bond formation to be rationalized and the correlation of the qualitative results with the experimental metal–metal distances. Cyclic polynuclear species, which appear to be a new expanding field in the chemistry of Pt–nucleobase complexes, are also described.

Keywords: Platinum complexes; Cisplatin; Nucleobase; Metal–DNA interaction

1. Introduction

The landmark discovery of the antitumor activity of *cis*-diamminedichloroplatinum(II) (cisplatin, cis-DDP) by Rosenberg et al. [1] some 25 years ago and early indications of Pt–DNA interactions playing a crucial role in the mode of action [2] have led to a large interest in all aspects of reactions of Pt coordination compounds with nucleic acids, oligonucleotides and models thereof. Views on the mode of action of antitumor Pt drugs have undergone changes over the years, from the simple concept that cisplatin coordination leads to a block in DNA replication and consequently cellular death to a more complex picture according to which cisplatin binding to DNA triggers a complicated cascade of events involving a series of players, namely gene products that sense the damage, signal it and eventually cause the cancer cell to die in a programmed fashion [3]. Cisplatin undergoes intracellular activation via Cl hydrolysis. The monofunctional adducts that form initially with DNA close to bis(nucleobase) adducts with a halflife of approx. 2 h [4]. Theoretically, a large number of possible bis(nucleobase) adducts can form with the four common DNA bases guanine (G), adenine (A), cytosine (C) and thymine (T): 10 bis(nucleobase) combinations are possible in theory, linkage isomers and multinuclear species (e.g. μ-OH or μ-nucleobase adducts; long range adducts; intra- vs. interstrand adducts) not considered. Monofunctional Pt binding does not appear to be sufficient to lead to antitumor activity in general, even though there are remarkable exceptions (e.g. complexes of type *cis*-$[(NH_3)_2PtLCl]^+$ L being a heterocyclic N donor such as cytosine or substituted pyridine [5]). By use of biochemical methods, the nature of the major adducts of cisplatin with DNA have been elucidated [6,7]. These are the intrastrand GG cross-link (50%–60%), followed by the intrastrand AG cross-link (20%–30%), the intrastrand GXG cross-link (10%), the

interstrand GG adduct (<1%) and DNA–protein cross-links (<1%). Nothing is known about any of the other minor adducts. Whether the abundance of a certain DNA adduct correlates with its significance in cytotoxicity is not really clear, even though it is frequently assumed to be so. Considering more recent findings on active Pt(II) and Pt(IV) compounds possessing a trans geometry of their amine ligands, this aspect will be increasingly important. Such compounds cannot (Pt(II)) or are unlikely (Pt(IV)) to form intrastrand GG or AG adducts and therefore must have a different spectrum of DNA cross-links. The cross-resistance of certain families of Pt drugs likewise points in a similar direction. These findings would seem to imply that there may be various Pt DNA adducts rather than a unique one triggering cellular destruction. The cisplatin–DNA cross-link studied most intensively — in fact almost exclusively — is the major one, *cis*-a_2PtGG. Many aspects of its formation, geometry and spectroscopy as well as its effect on DNA structure and function have been studied at a high degree of sophistication [8–14]. It is the only cisplatin adduct to date which has been crystallized and its crystal structure determined by X-ray methods on the di- [8] and trinucleotide [9] level. Essential structural features such as head–head orientation of the two bases, dihedral angles or deviations of Pt from guanine planes had also been derived from simple 9-ethylguanine model compounds, however [15,16]. In this article we review X-ray structural work on Pt compounds containing simple model nucleobases. In many cases the X-ray structure determination was not specifically undertaken to shed light on questions related to the geometry of the complex but rather to complement and support conclusions on the basic chemistry of such compounds. A wealth of information has emerged this way over the years [17–19].

2. Mononuclear Pt(II) complexes

A great number of platinum(II) complexes with monodentate nucleobases forming square planar coordination units have been investigated in the past several years. The complexes so far structurally characterized contain one or two nucleobases while the other coordination positions about Pt are mainly occupied by Cl, and/or ligands containing N donors. Only one structural characterization of a complex containing three cytosines [20] and a preliminary report on a tetrakis(9-methylguanine) complex of Pt(II) [21] have been reported.

In many cases these complexes are considered models for possible DNA–cisplatin interaction, and therefore the pyrimidine (pym) nucleobases are generally Me-substituted in position 1 and the purine (pu) bases are Me- or Et-substituted in position 9. Thus the deoxyribose moiety of the DNA nucleosides is replaced by an alkyl group and metal coordination at these N sites is prevented.

However, there are also examples in which the nucleobase is underivatized or alkylated in other positions. Since the nucleobases as monodentate ligand, both in neutral or ionic forms, may coordinate in different ways, different linkage isomers can be obtained. The formula of the substituted nucleobases, labelled according to a unified symbolism, are shown in Fig. 1 and Fig. 2. These labels are used throughout

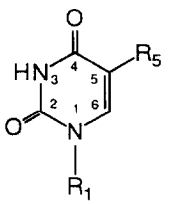

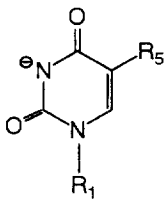

		R_1	R_5
UH_2	UH^-	H	H
1-MeUH	1-MeU^-	Me	H
TH_2	TH^-	H	Me
1-MeTH	1-MeT^-	Me	Me

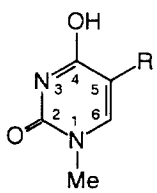

4-H, 1-MeUH
4-H, 1-MeTH (R=Me)

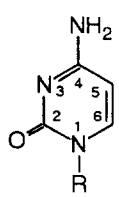

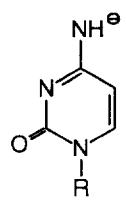

C	R = H	1-MeC^-
1-MeC	R = Me	

Fig. 1. Numbering scheme and formula of neutral and deprotonated pyrimidine nucleobases.

the review, followed by the indication of the donor atom(s) bonded to the metal centre.

Structural data were obtained from structures retrieved in the version 5.08 of October 1994 of the Cambridge Structural Database (CSD) [22]. In addition, few examples of recent data not yet implemented in the CSD will be mentioned.

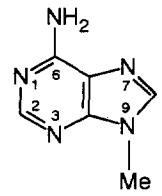

9-MeA

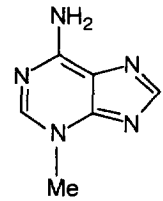

3-MeA

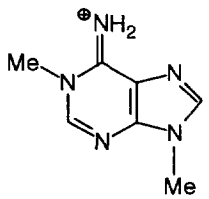

$1,9\text{-Me}_2\text{AH}^+$

$6,9\text{-Me}_2\text{AH}^+$

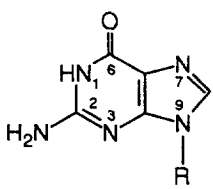

9-RGH

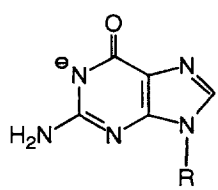

9-RG^-

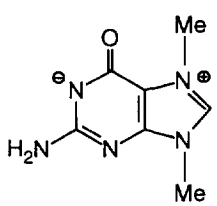

2.1. Mono(nucleobase) complexes

The compounds so far structurally characterized are reported in Table 1 together with coordination bond lengths, displacements of Pt from the coordination plane, *d*, and the angle between the coordination and nucleobase mean planes, and they are identified by the CSD reference code (Refcode).

In complexes containing a pym base, neutral forms of cytosine (C) and 1-methylcytosine (1-MeC) are always coordinated through N3, as well as the N3 deprotonated 1-MeU$^-$ (or 1-MeT$^-$). For the (unsubstituted) uracil or thymine anion, UH$^-$ or TH$^-$ [47], the binding site is preferentially N1 [36]. However, the N3 linkage isomer of a Pt(II) complex containing UH$^-$ has also been crystallized recently [37].

The square planar coordination of Pt is characterized by small values of *d*, which range from 0.001 to 0.052 Å, whereas the dihedral angle ranges from 72° to 89°, with the exception of two structures involving uracilate [(UH$^-$,N^1)Pt(en)Cl] and thyminate anions [(TH$^-$,N^1)Pt(en)Cl] where this angle is 50° and 56°, respectively (Table 1). Hydrogen bonding is believed to be of fundamental importance in determining the angle in the cited structures [36].

There is no apparent relationship between α angles and Pt–N(pym) bond lengths (ranging from 1.973 to 2.059 Å). The largest values for distances are found for 1-MeC,N3 trans to S(O)(i-Pr)$_2$, (2.058(7) Å) [26] and for 1-MeT$^-$,N^3 trans to a phosphine ligand (2.06(2) Å) [35]. The lengthening can be attributed to the greater trans influence of the S and P donor, compared with N donors.

As far as purine complexes are concerned, the monodentate guanine ligand in its neutral form coordinates through N7, since N1 is protonated and N3 site is less basic and, probably, more sterically hindered. Numerous solution studies confirm this view [17]. Only the modified purine base 7,9-Me$_2$G (Fig. 2) coordinates through N1, because position 7 is methylated. Analogously, in the majority of structurally characterized adenine complexes of Pt(II), the metal coordination site is N7, with only one example known for N1 binding [38]. If the 9-MeA ligand is protonated (at N1), Pt binding is as expected through N7 [40].

In these mononuclear purine complexes deviation of Pt from the mean plane of the four donor atoms ranges from 0.003 to 0.062 Å. The α angles and the Pt–N(pu) distances range from 62 to 81° and from 2.000 to 2.044 Å, respectively, but no apparent relationship can be derived between these geometrical parameters.

In the *trans*-[(9-(2-acetoxyethoxyMe)GH,N^7)PtCl$_2$(CH$_2$=CH$_2$)] the α angle is reduced noticeably (45°) and the distance Pt–N(GH) is the longest reported (2.078(3) Å), suggesting for the latter a significant trans influence of the ethylene molecule [45].

The Pt–N1(pu) distances turn out to be slightly longer than the Pt–N7(pu) ones and are very close to the typical distances found in Pt–N(pym) derivatives of Table 1. This difference could be ascribed to the endocyclic C–N$_c$–C angle (N$_c$ being the donor site), narrower in the five membered rings than in the six-membered ones, which allows a closer approach of the ligand to the metal centre. Correspondingly

Table 1
Mononuclear complexes (nb)Pt(II)L_3

Config. nb L1 L2 L3 (L2 trans to nb)	Refcode	Pt–nb	Pt–L1	Pt–L2	Pt–L3	*d*	α	Ref.
Pyrimidine bases								
cis 1-MeC,N^3 NH_3 NH_3 OH	BAGKOJ10	2.034	2.022	2.036	2.028	0.009	79.7	[23]
cis 1-MeC,N^3 NH_3 NH_3 H_2O	BAGKUP10	2.036	2.023	2.034	2.027	0.005	89.4	[23]
cis 1-MeC,N^3 NH_3 NH_3 Cl	CTSPTA	2.024	2.074	2.046	2.299	0.014	88.1	[24]
	CTSPTA01	2.058	2.051	2.039	2.299	0.011	84.0	[24]
	DUJNIF	2.018	2.104	2.048	2.291	0.014	83.4	[25]
trans 1-MeC,N^3 Cl S(O)iPr_2 Cl	IPSMCP	2.059	2.302	2.231	2.289	0.022	83.9	[26]
cis 1-MeC,N^3 (Me_4en) Cl	JEHPOB	2.039	2.079	2.066	2.335	0.004	86.9	[27]
trans 1-MeC,N^3 Cl NH_3 Cl	MCSPTA	2.030	2.288	2.044	2.296	0.009	72.1	[28]
trans 1-MeC,N^3 NH_2Me (Gly,N) NH_2Me	VEPROX	2.044	2.053	2.061	2.057	0.001	80.3	[29]
cis 1-MeC,N^3 NH_3 NH_3 (Gly,N)	VOLCUU	2.015	2.033	2.025	2.055	0.034	71.8	[30]
trans 1-MeC,N^3 NH_2Me Cl NH_2Me	VEPRUD	2.036	2.072	2.291	2.061	0.011	81.5	[29]
1-MeC,N^3 [$NH_2(CH_2)_2NCHCH_2NH_2$]	VEZMES	2.024	2.039	1.955	2.063	0.000	74.1	[31]
C,N^3 Cl Cl Cl	GIFWAT	2.049	2.298	2.309	2.305	0.001	75.7	[32]
cis C,N^3 NH_3 NH_3 Cl	KABJUS	2.033	2.059	2.045	2.309	0.016	79.8	[33]
cis 1-MeT$^-$,N^3 NH_3 NH_3 Cl	DEYXUA	1.973	2.052	2.002	2.326	0.012	76.5	[34]
cis 1-MeT$^-$,N^3 [PPh_2Cp-Fe-CpPh_2P] $OCHNMe_2$	VOYRIK	2.055	2.237	2.266	2.137	0.046	75.2	[35]
TH$^-$,N^1 Cl (en)	CTYEPT	2.036	2.298	2.033	2.038	0.052	55.8	[36]
UH$^-$,N^1 Cl (en)	CTYEPU	2.034	2.298	2.021	2.032	0.022	50.0	[36]
UH$^-$,N^1 (en) H_2O	*	2.019	2.009	2.049	2.067		74.0	[37]
UH$^-$,N^3 NH_3 NH_3 Cl	*	2.038	1.999	2.028	2.280			[37]
Purine bases								
9-MeA,N^1 (dien)	SISCIG	2.043	2.043	2.021	2.032	0.062	65.9	[38]
7,9-Me_2G,N^1 (dien)	BAHNUT	2.044	2.060	2.020	2.034	0.027	62.3	[39]
9-MeAH$^+$,N^7 Cl Cl Cl	CMADPT	2.015	2.301	2.302	2.297	0.008	62.4	[40]
9-MeA,N^7 NH_3 NH_3 NH_3	DEGJUU	2.000	2.016	2.022	2.052	0.026	69.9	[41]
cis 1,9-Me_2AH$^+$,N^7 Cl Cl NH_3	JUNPUD	2.002	2.321	2.283	2.048	0.009	76.9	[42]
6,9-Me_2AH$^+$,N^7 Cl Cl Cl	JUNRAL	2.009	2.306	2.286	2.287	0.011	66.9	[42]
9-MeGH_2^+,N^7 Cl Cl Cl	BINCOQ10	2.010	2.305	2.292	2.301	0.026	79.1	[43]
trans (N,N′-Me_2 9-MeGH,N^7) NH_3 NH_3 Cl	BOHDAD	2.034	2.059	2.027	2.300	0.003	81.4	[44]
trans 9-(2-AcetoxyethoxyMe)GH,N^7 Cl (CH_2=CH_2) Cl	SOFYOB	2.078	2.302	2.143 2.150	2.291	0.045	44.7	[45]
(7-deaza-8-aza)9-MeA,N^1 (dien)	JONLAZ	1.937	2.127	1.918	2.108	0.056	88.7	[46]

Bond lengths and angles are reported with four and three significant digits. Readers should address the reference for the uncertainty of these parameters. Values retrieved from original papers are indicated by an asterisk (*) before the Refcode (no atoms coordinates or errors detected in CSD files). An * also indicates a new structure not implemented in CSD yet.

Table 2
Mononuclear complexes $(nb)_2Pt(II)L_2$

Config. nb1 nb2 L1 L2	Refcode	Pt–nb1	Pt nb2	Pt–L1	Pt–L2	*d*	$\phi 1$	$\phi 2$	β	Ref.
Bis(pyrimidine)										
cis 1-MeC,N^3 1-MeC,N^3 NH_3 NH_3	BARZOJ	2.031	2.040	2.031	2.033	0.025	103	107	77.7	[48]
	BARZOJ01	2.033	2.044	2.049	2.055	0.025	103	107	78.0	[49]
	DUJNOL	2.042	2.010	2.036	2.021	0.020	107	105	84.3	[25]
cis 1-MeC,N^3 1-MeC,N^3 (Me_4en)	JIKGEP	2.049	2.049	2.044	2.044	0.000	96	96	88.9	[50]
cis 1-MeC,N^3 1-MeC,N^3 (bmik)	*	2.049	2.035	2.024	2.025				80.0	[51]
cis (4H,1-MeTH,N^3) 1-MeT$^-$,N^3 NH_3 NH_3	JONLED	2.039	2.045	2.054	2.062	0.022	81	−88	72.9	[52]
cis 1-MeT$^-$,N^3 1-MeT$^-$,N^3 $NH_2CH(CH)_2$ $NH_2CH(CH)_2$	KELMAP	2.059	2.037	2.063	2.043	0.049	−77	108	83.6	[53]
cis 1-MeU$^-$,N^3 1-MeU$^-$,N^3 NH_3 NH_3	BOSSOR	2.033	2.050	2.057	2.051	0.000	111	119	70.7	[54]
cis 1-MeU$^-$,N^3 (4H,1-MeUH,N^3) NH_3 NH_3	SEBVEA	2.035	2.040	2.048	2.041	0.008	−96	114	69.5	[55]
cis (4H,1-MeUH,N^3)(4H,1-MeUH,N^3) NH_3 NH_3	SEBVIE	2.047	2.008	2.023	2.032	0.010	120	112	82.2	[55]
cis 1-MeC,N^3 TH$^-$,N^1 NH_3 NH_3	BAPKAE	2.025	2.040	2.035	2.082	0.008	117	108	82.6	[56]
	*MCTHPT	2.02	1.90							[57]
cis 1-MeC,N^3 1-MeT$^-$,N^3 [PPh_2Cp-Fe-CpPh_2P]										
(bases not differentiated)	*VOYRUW	2.10	2.10	2.274	2.274					[35]
trans 1-MeC,N^3 1-MeC,N^3 NH_3 NH_3	GEBVUE	2.028	2.028	2.055	2.055	0.000	180	–	0.0	[58]
	MCSPTB	2.026	2.026	2.060	2.060	0.000	180	–	0.0	[28]
Bis(purine)										
cis 9-MeG$^-$,N^1 9-MeG$^-$,N^1 (en)	KUKGUS	2.061	2.046	2.046	2.044	0.053	61	67	76.7	[59]
cis 3-MeA,N^7 3-MeA,N^7 NH_3 NH_3	BILROD	2.010	2.003	2.038	2.031	0.022	79	67	89.4	[60]
cis 9-MeA,N^7 9-MeA,N^7 NH_3 NH_3	JISMUT	2.013	2.022	2.042	2.050	0.005	83	87	89.2	[61]
cis 9-EtGH,N^7 9-EtGH,N^7 NH_3 NH_3	CUHJIY	2.029	2.023	2.047	2.040	0.006	−99	46	68.2	[15]
	CUHJOE	2.025	2.017	2.051	2.036	0.011	49	−101	70.3	[15]
	DEGXAO	1.963	2.010	1.969	2.047	0.033	−49	95	75.4	[62]
	DEGXES	2.024	2.002	2.044	2.043	0.002	−115	66	78.0	[62]
cis 9-EtGH_2^+,N^7 9-EtGH_2^+,N^7 Cl Cl	SEWDUV	2.025	2.006	2.269	2.292	0.054	130	119	57.6	[63]
cis 9-EtGH,N^7 9-EtGH,N^7 $NH_2(CH_2)_2$Me $NH_2(CH_2)_2$Me	SEWFAB	2.032	2.008	2.054	2.031	0.018	45	56	64.1	[63]
cis 9-MeGH,N^7 9-MeGH,N^7 (Me_4en)	GEHGOP	2.017	2.018	2.075	2.056	0.016	80	97	80.9	[64]
cis 9-EtGH,N^7 9-EtGH,N^7 (Me_4en)	GEHGUV	2.016	2.004	2.059	2.042	0.003	89	94	88.2	[64]
cis 9-MeGH,N^7 9-MeGH,N^7 (bmik)	*	2.005	2.002	2.004	1.995				89.0	[51]

cis 9-MeGH,N^7 9-MeGH,N^7 PMe_3 PMe_3	*	2.10	2.11	2.255	2.246	0.19			77.6	[65]
trans 9-EtGH,N^7 9-EtGH,N^7 NH_2Me NH_2Me	JUJFID	2.020	2.020	2.033	2.033	0.000	180	–	0.0	[66]
(Pyrimidine)(purine)										
cis 1-MeC,N^3 9-MeA,N^7 NH_3 NH_3	DODLAJ	2.049	2.013	2.029	2.043	0.023	−94	−85	88.2	[67]
cis 1-MeC,N^3 9-EtGH,N^7 NH_3 NH_3	CYTPTA10	2.031	2.016	2.056	2.047	0.020	90	80	76.4	[68]
		2.038	2.013	2.068	2.075	0.036	97	86	77.8	
cis 1-MeC,N^3 9-EtG^-,N^7 NH_3 NH_3	CYTPTD10	2.004	2.017	2.058	2.064	0.020	104	−82	83.3	[68]
cis 1-MeC,N^3 9-EtGH/9-EtG^-,N^7 NH_3 NH_3	MCPTEG10	2.014	2.050	2.045	2.059	0.040	−117	−73	80.7	[68]
trans 1-MeC,N^3 9-MeA,N^7 NH_3 NH_3	DODLEN	2.031	2.008	2.068	2.060	0.027	−177	–	2.6	[67]
trans 1-MeC,N^3 9-MeGH,N^7 NH_2Me NH_2Me	JOMCOD	2.050	2.011	2.039	2.046	0.032	1	–	9.9	[69]
trans 1-MeT^-,N^3 9-MeA,N^1 NH_2Me NH_2Me	YATSUH	2.030	2.051	2.054	2.044	0.048	9	–	16.4	[70]
trans 1-MeT^-,N^3 9-MeA,N^7 NH_3 NH_3	YATTES	2.018	2.022	2.029	2.074	0.034	−3	–	4.3	[70]
		1.999	2.014	2.028	2.039	0.014	−8	–	11.9	
trans 2-NH_2py 9-MeGH,N^7 NH_3 NH_3	YATTAO	2.011	2.009	2.037	2.036	0.029	−18	–	14.3	[70]

the two C–N_c–Pt angles are significantly smaller when N_c belongs to a six-membered ring (see Section 9).

2.2. Bis(nucleobase) complexes

Structural details of bis(nucleobase) complexes, namely coordination distances, displacements *d* and dihedral angles between the two nucleobase mean planes, β, are reported in Table 2. The species so far structurally characterized can be grouped in bis(pyrimidine), bis(purine), and mixed (purine)(pyrimidine) complexes. The other two ligands completing the metal coordination are identical and mainly contain N donors.

In order to define the solid state conformational features of the two nucleobases in cis isomers, the torsional angles $\phi 1$ and $\phi 2$ about the respective N(nb)–Pt bonds are also reported in Table 2. The latter parameters allow a fair quantitative definition of the orientation of the base rings with respect to the coordination plane and of the mutual orientation of the base rings. The proposed convention reports the torsional angles C2–N3(nb1)–Pt–N3(nb2) ($\phi 1$) and C2–N3(nb2)–Pt–N3(nb1) ($\phi 2$) for pyrimidine and purine bases N3 coordinated, as depicted in Fig. 3 and C8–N7(nb1)–Pt–N7(nb2), C8–N7(nb2)–Pt–N7(nb1) for purine N7 coordinated [71]. The value of angle $\phi 1$ (or $\phi 2$) defines the amount of the clockwise (+) or counterclockwise (−) rotation around their respective Pt–N(nb) coordination bond. Thus, when the reference atoms (C2 or C8) bonded to the Nc–donor are on the same side of the coordination plane in a head–head (h-h) arrangement, $\phi 1$ and $\phi 2$ have values with opposite sign. They agree in sign for a head–tail (h-t) conformation. Further, the $\phi 1$ and $\phi 2$ angles measure approximately the two dihedral angles between each nucleobase and the coordination plane, being both $+90°$ for two nucleobases perpendicular to the coordination plane in a h-t arrangement (as sketched in Fig. 3(a)). For *cis*-$(nb)_2Pta_2$ species, two enantiomers (atropisomers) are possible for the h-t orientation, and this aspect has been investigated by using NMR spectroscopy on bis(nucleoside) [72] and bis(nucleotide) complexes [73].

It is of interest to note that for cis isomers, where $\phi 1$ and $\phi 2$ angles present quite a variable range (i.e. orientation of nucleobases with respect to the coordination plane), the β angles (i.e. the mutual orientation of the two nucleobases) are almost similar.

In order to define the mutual orientation of the two bases, in trans isomers, one value is reported, namely the virtual torsional angle C2–N3(nb1)·N3(nb2)–C2 (Fig. 3(b)).

The same scheme also applies to cis and trans mixed (purine)(pyrimidine) complexes.

Although a different stereochemical approach has been proposed some years ago by Kistenmacher and coworkers [48,74] for comparing the primary conformational aspects of *cis*-$[(nb)_2Pta_2]$ type complexes, the present convention appears simpler and easy to visualize.

As evident from Table 2, the large majority of bis(nucleobase) complexes of Pt(II) studied by X-ray diffraction have a cis geometry and both h-h and h-t arrangements

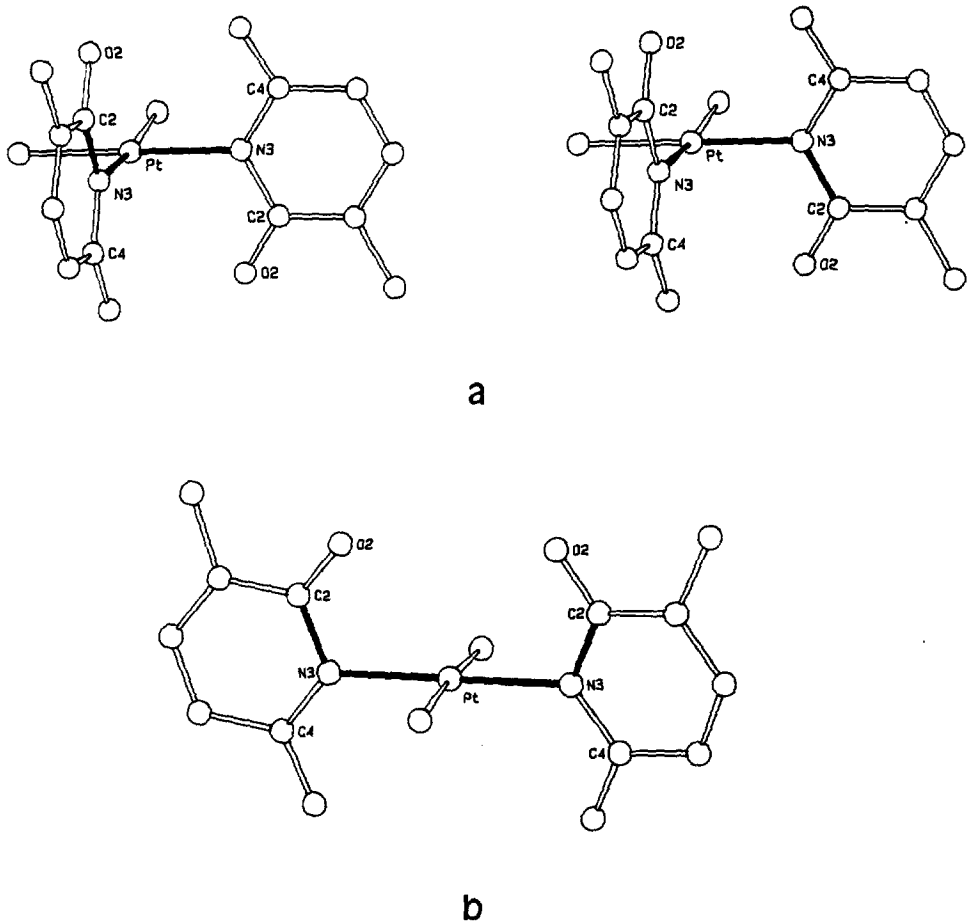

Fig. 3. Torsional angles $\phi 1$ and $\phi 2$ defining the bases conformation in *cis*- and *trans*-$[(nb)_2Pta_2]$ complexes.

are found, as shown by the sign of angles $\phi 1$ and $\phi 2$. The trans isomers of the first two groupings possess a crystallographic symmetry center, so that the two nucleobases definitely have a h-t arrangement.

However, for bis(pyrimidine) complexes the h-t arrangement is generally predominant and the h-h one requires stabilization either by intramolecular H bonding, as it occurs in SEBVEA [55] and JONLED [52] between O4 of the 1-methyluracilato (or 1-methylthyminato) anion and HO4 of the neutral iminol form of the respective nucleobase, or by intermolecular H bonding (see infra). In fact, the crystal structure determinations of *cis*-$[(4\text{-H},1\text{-MeUH})_2Pt(NH_3)_2]^{2+}$, *cis*-$[(1\text{-MeU}^-)(4\text{H},1\text{-MeUH})\text{-}Pt(NH_3)_2]^+$ [55], and *cis*-$[(4\text{-H},1\text{-MeTH})(1\text{-MeT}^-)Pt(NH_3)_2]^+$ [52] complexes reveal the neutral pyrimidine ligands in the 2-oxo-4-hydroxo form (Fig. 1). These rare iminol tautomers of 1-methyluracil or 1-methylthymine are stabilized upon coordination to the metal. On the basis of these results, a model for a metal-assisted

tautomerization of 1-MeUH has been proposed which could model certain mutagenic transitions in DNA [55]. The only other examples of Pt(II) complexes with h-h arranged pyrimidine nucleobases have been observed with *trans*-$[(MeNH_2)_2Pt(1\text{-}MeC)_2]X_2$ (X is ClO_4^- or PF_6^-) [75]. Although this compound, when isolated from aqueous solution upon slow evaporation, displays a h-t orientation of the two cytosines nucleobases (very much as the NH_3 analogues GEBVUE and MCSPTB), the respective h-h rotamer can be isolated from aqueous solution upon treatment of its heteronuclear derivatives (see Section 4.1.3.) with suitable nucleophiles and rapid crystallization of the parent compound in its h-h form. In the course of this work it has also been found that DMSO and DMF strongly favor the h-h over the h-t rotamer in solution. This finding suggests that crystallization from different solvents may have a marked effect on nucleobase orientation in the solid state.

For bis(purine) complexes, the two bases are also usually oriented head–tail, leading approximately to a C_2 molecular symmetry. The only exception, namely a head–head arrangement of two guanines, is found in *cis*-$[(9\text{-}EtGH,N^7)_2Pt(NH_3)_2]^{2+}$. This complex has been crystallized with four different counterions [15,62]. The h-t arrangement has also been observed in $[(9\text{-}MeG^-,N^1)_2Pt(en)]$ where the deprotonated guanines coordinate through N1 [59]. Since the h-t arrangement of two adjacent guanine bases seems to be rather unlikely in native DNA, the relevance of most bis(guanine) structures as models for a GG cross-link may be questioned for this reason [62]. The structural results seem to be in agreement with the suggestion that the h-t arrangement of the two bases may be the thermodynamically most stable conformation [76]. A molecular mechanics analysis for *cis*-$[(pu)_2Pta_2]$ complexes, with a_2 being small amine ligands, showed that differences in interactions between the purine and the amine ligands are almost entirely responsible for the energy barriers of rotation. The calculated values are less than 30 for guanine and greater than 40 kJ mol^{-1} for adenine ligands N7 coordinated [77]. In contrast, from NMR spectroscopy, rotational activation energies for a series of *cis*-$[(6\text{-aminopurine})_2Pt(NH_3)_2]$ lie in the range 46–95 kJ mol^{-1}; a lower barrier of 25 kJ mol^{-1} is exhibited by a complex containing bis(6-oxopurine) [73b].

A common structural feature of *trans*-$[(pu)(pym)Pta_2]$ complexes is the approximately coplanar arrangement ($\beta = 2.6$–$16.4°$) of the two nucleobases due to direct or indirect (via a water molecule) intramolecular H bond between the two bases [67,69,70]. These complexes, with two heterocyclic ligands, have been proposed as models for temporary or permanent cross-linking products of metal ion with two nucleic acid strands ("metal-modified base pairs") [78]. For example, two complementary bases are arranged in a Watson–Crick fashion in *trans*-$[(1\text{-}MeT^-,N^3)(9\text{-}MeA,N^1)Pt(NH_3)_2]^+$ (YATSUH) or in a Hoogsten base pairing in *trans*-$[(1\text{-}MeT^-,N^3)(9\text{-}MeA,N^7)Pt(NH_3)_2]^+$ (YATTES) [70].

Despite the variations in the Pt–N(nb) bond lengths in mono(nucleobase) and (bis)nucleobase complexes reported in Tables 1 and 2, the mean values follow the same trend:

Pt–N7(pu)	<	Pt–N3(pym)	~	Pt–N1(pym)	<	Pt–N1(pu)
2.015(2)		2.034(2)		2.032(5)		2.041(5) Å

This is also documented by the four independent structural investigations [15,62] of *cis*-[(9-EtGH,N^7)$_2$Pt(NH_3)$_2$]$^{2+}$, where the Pt-N7 distances average to 2.010 Å, of *cis*-[(9-MeG$^-$,N^1)$_2$Pt(en)], where the Pt–N1 mean distance is 2.054 Å [59], of *cis*-[(1-MeC,N^3)$_2$Pt(NH_3)$_2$]$^{2+}$, where the Pt–N3 average is 2.033 Å [25,48,49].

The angles about the N donor of the base show values similar to those observed in mono(nucleobase) complexes. The mean values of Pt–N–C angles are reported later (see Section 9.3.).

The Pt–N3(pym) distances should be compared with those of 2.008(5) and 2.014(7) Å reported for the two complexes containing the parent pyrimidine, namely *trans*-[(pyrimidine,N^3)$_2$PtX$_2$] where X is Cl and Br [79], respectively. This suggests that the presence of α-substituents with respect to the N donor atom, could also contribute to a lengthening of the Pt–N bond, and to effect the value of angle α. In the latter species the observed values are 52.5 and 54.3°, respectively.

A fair linear relationship has been observed when angles are plotted against the C5–N7–Pt bond angles [45]. Fig. 4 reports a typical plot for 29 guanine bases with a correlation factor of 0.747. However, the trend in 6-oxopurines is more

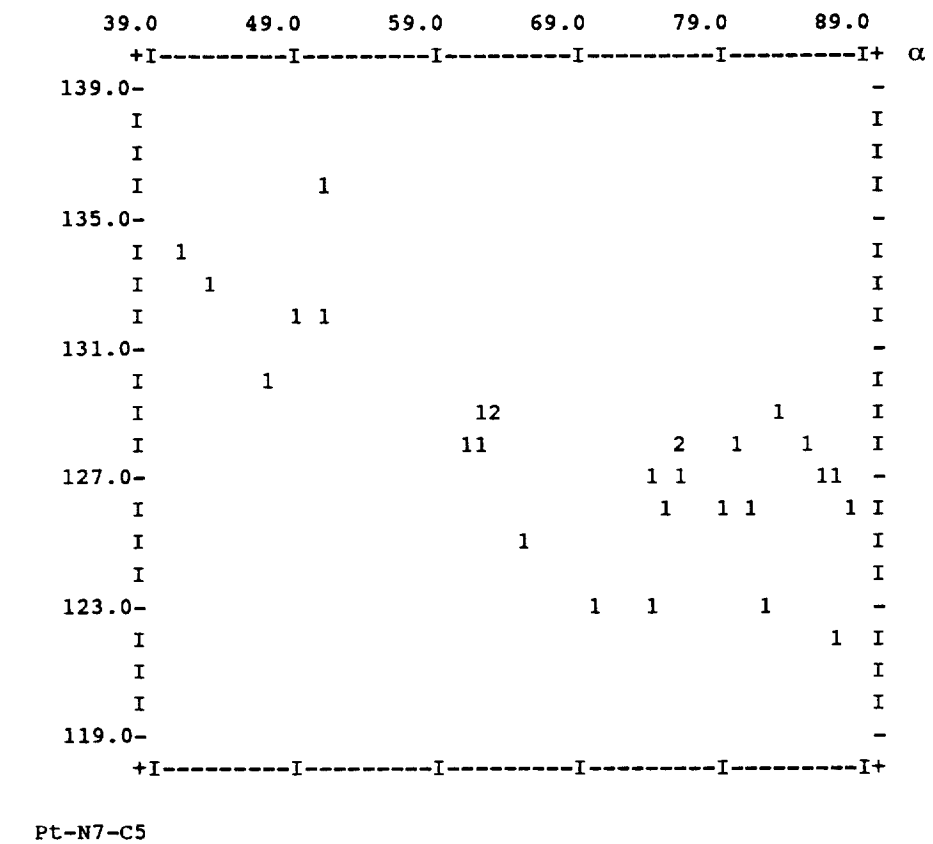

Fig. 4. Plot of angle α against the Pt–N7–C5 bond angle for guanines N7 coordinated.

complex, as shown by L. Marzilli et al. [14], which analyzed the rocking angle, i.e. Δ=(C5–N7–Pt)–(C8–N7–Pt), as a function of the torsional angle around the Pt–N7 bond (τ). They have found that for a conformation where the guanine is perpendicular to the Pt coordination plane ($\tau=90°$), the rocking angle is small, while large deviations from $\tau=90°$ correspond to larger Δ values, because of the steric interactions between O6 and the cis ligands, causing the lopsided base to bend away.

2.3. Tris(nucleobase) complexes

In the only structurally characterized example of a Pt(II) complex containing three cytosine nucleobases $[(1\text{-MeC},N^3)_3Pt(NH_3)]^{2+}$, the bases are forced to be mutually perpendicular, in order to minimize steric repulsions, with a Pt–N3 mean distance of 2.049 Å. The two trans cytosines have a h-h arrangement, whereas the cis cytosine exihibits an opposite (h-t) orientation [20]. Intermolecular H-bonding requirements were suggested as a possible reason for this arrangement. However, the structure of the Pd analogue has been obtained with significantly better accuracy. This allows the determination of more precise non-bonded distances, which strongly indicate that the conformation is stabilized by intramolecular H-bonding [80].

3. Mononuclear Pt(IV) complexes

Compared to Pt(II) compounds, a relatively small number of Pt(IV) compounds have been studied so far [81]. However, renewed interest in Pt(IV) antitumor compounds and the yet unsolved question of how interactions of Pt(IV) compounds with DNA occurs, is likely to produce more structural work in the future. In fact a particularly intriguing aspect of the biorelevant chemistry of Pt(IV) complexes is the question of drug activation through a possible in vivo reduction to Pt(II) [81 and refs. cited therein].

3.1. Mono(nucleobase) complexes

Some geometrical parameters for mono- and bis(nucleobase) Pt(IV) compounds are reported in Table 3.

The first examples of 1-methyluracil derivatives containing an octahedrally coordinated Pt(IV), have been reported in 1984, obtained through an oxidative addition of Cl_2 to Pt(II) complexes [82]. The structural features of the two compounds, of type *mer*-$[(rU^-,N^3)Pt(NH_3)_2Cl_3]$, where rU^- represents an uracilate derivative [86], are dictated by steric restraints imposed by the three mer Cl ligands and the two exocyclic oxygens O2 and O4 of the base. Consequently, dihedral angles between the base and the $PtCl(NH_3)_2$(N3) plane (N3 is the pym donor atom) are substantially reduced as compared to typical Pt(II) compounds, to values of 41° and 61°.

In the Pt(IV) complex containing a purine base, *mer,trans*-$[(9\text{-MeGH},N^7)$-$Pt(OH)_2(dien)]^{2+}$, the guanine plane is at a 57° angle relative to the PtN_4 plane

Table 3
Mononuclear Pt(IV) complexes

Config. nb L1 L2 L3 L4 L5 (L1 ligand trans to nb)	Refcode	Pt–nb	Pt–L1	Pt–L2	Pt–L3	Pt–L4	Pt–L5	$d1^a$ $d2^a$	α1 α2	Ref.
(nb)Pt(IV)L_5										
mer (5-Cl,1-MeU$^-$,N^3) NH_3 NH_3 Cl Cl Cl	CUVBIE	2.140	2.056	2.061	2.315	2.311	2.316	0.002	41.0	[82]
								0.014	53.1	
		2.089	2.049	2.083	2.330	2.321	2.311	0.042	41.4	
								0.018	55.5	
mer(5,5-Cl_2,6-OH,5,6-H_2,1-MeU$^-$,N^3) NH_3 NH_3 Cl Cl Cl	CUVBOK	2.076	2.081	2.054	2.334	2.324	2.315	0.017	61.4	[82]
								0.028	36.7	
mer,trans 9-MeGH,N^7 (dien) OH OH	JUCMAV	2.051	2.016	2.029	2.057	1.999	1.989	0.018	56.7	[83]
								0.026	33.8	
Config. nb1 nb2 L1 L2 L3 L4	Refcode	Pt–nb1	Pt–nb2	Pt–L1	Pt–L2	Pt–L3	Pt–L4	β	ϕ	Ref.
$(nb)_2Pt(IV)L_4$										
trans,trans,trans 1-MeC,N^3 1-MeC,N^3 NH_3 NH_3 OH OH	FEGBUO	2.060	2.060	2.059	2.059	2.006	2.006	0.0	180	[81]
trans,trans 1-MeC,N^3 1-MeC,N^3 NH_3 NH_3 H_2O OH	FEGCAV	2.073	2.082	2.050	2.072	2.064	1.981	20.9	0	[81]
trans 1-MeC,N^3 1-MeC$^-$,N^3,N^4 OH NH_3 NH_3	FEGCEZ	2.066	1.969	2.032	2.033	2.076	2.111	35.1	161	[81]
trans,trans 1-MeC ,N^3,N^4 1-MeC$^-$,N^3,N^4 NH_3 NH_3	DAXNUL10	2.037	2.038	2.037	2.038	2.058	2.058	0.0	180	[81]
trans,trans,trans 1-MeUH,N^3 1-MeUH,N^3 NH_3 NH_3 OH OH	KETDAO	2.080	2.080	2.061	2.061	1.987	1.987	0.0	180	[84]
trans,trans,trans 1-MeC,N^4 1-MeC,N^4 NH_3 NH_3 OH OH	FATPAR	2.028	2.028	2.049	2.049	2.003	2.003	0.0		[85]
trans,trans,trans 1-MeC,N^4 1-MeC,N^4 NH_3 NH_3 OH OH	FATPAR01	2.022	2.022	2.042	2.042	2.008	2.008	0.0		[85]

[a] *d1* out of plane 1 = nb, L1, L2, L3; *d2*, of plane 2 = nb, L1, L4, L5.

(containing the N donors of dien ligand) [83]. The guanine oxygen is involved in a hydrogen bond (2.744(7) Å) with one of the two axial OH ligands of the metal.

3.2. Bis(nucleobase) complexes

Several octahedral Pt(IV) complexes containing two nucleobases have been obtained as oxidation products from *trans*-$[(1\text{-MeC},N^3)_2Pt(NH_3)_2]^{2+}$ [81–85].

The cations *trans,trans,trans*-$[(1\text{-MeC},N^3)_2Pt(NH_3)_2(OH)_2]^{2+}$ (FEGBUO) and *trans,trans*-$[(1\text{-MeC},N^3)_2Pt(NH_3)_2(H_2O)(OH)]^{3+}$ (FEGCAV) possess ligands (OH, NH_3, H_2O) which have been identified on the basis of the expected different hydrogen bonding properties [81].

The first cation is centrosymmetrical, leading to an all-trans arrangement of the different types of ligands. The Pt–NH_3 distances do not differ from those observed in the precursor of Pt(II), *trans*-$[(1\text{-MeC},N^3)_2Pt(NH_3)_2]^{2+}$ [28,58], whereas the Pt–N(pym) distances are appreciably longer, by about 0.04 Å compared with the Pt(II)–N(pym) bond lengths.

The corresponding linkage isomer *trans,trans,trans*-$[(1\text{-MeC},N^4)_2Pt(NH_3)_2(OH)_2]^{2+}$, where 1-MeC is bonded to Pt by N4, can be obtained from complex FEGBUO, through two stable intermediates, resulting from a facile interconversion of one or both the monodentate 1-MeC,N^3 ligands bound to Pt via N3, to chelating deprotonated 1-MeC^-,N3,N4 ligands, i.e. the monochelate *trans,trans*-$[(1\text{-MeC},N^3)(1\text{-MeC}^-,N^3,N^4)Pt(NH_3)_2(OH)]^{2+}$ and the bischelate *trans,trans*-$[(1\text{-MeC}^-,N^3,N^4)_2Pt(NH_3)_2]^{2+}$, respectively.

In *trans,trans*-$[(1\text{-MeC},N^3)(1\text{-MeC}^-,N^3,N^4)Pt(NH_3)_2(OH)]^{2+}$, the Pt–N3 distances of the neutral 1-MeC coordinated through N3 and of 1-MeC^- anion (chelating via N3 and N4) are different, being 2.03(2) and 1.97(1) Å, respectively [81]. On the contrary, the Pt–N3 and Pt–N4 distances in *trans,trans*-$[(1\text{-MeC}^-,N^3,N^4)_2Pt(NH_3)_2]^{2+}$ [81], where the 1-MeC^- coordinate Pt through N3 and the exocyclic amino group N4, are equal, being 2.037(9) and 2.04(1) Å, respectively. As the latter cation is centrosymmetric, the bases are coplanar with opposite orientation (h-t).

In *trans,trans,trans*-$[(1\text{-MeC},N^4)_2Pt(NH_3)_2(OH)_2]^{2+}$, the 1-MeC ligands are in the rare iminooxo tautomer form of cytosine, protonated at N3 and coordinated to Pt through the deprotonated exocyclic N4.

The cation *trans,trans,trans*-$[4H,1\text{-MeUH})_2Pt(NH_3)_2(OH)_2]^{2+}$ [84], has been obtained starting from *trans*-$[(1\text{-MeU}^-)_2Pt(NH_3)_2]$. The correct formulation for this Pt(IV) species is ambigous because of the difficulty in locating the acidic protons directly. Alternative descriptions such as *trans,trans,trans*-$[(1\text{-MeU}^-)_2Pt(NH_3)_2(OH_2)_2]^{2+}$ or *trans,trans*-$[(4\text{-H},1\text{-MeUH})(1\text{-MeU}^-)Pt(NH_3)_2(OH)(OH_2)]^{2+}$ are feasible.

4. Dinuclear complexes

4.1. Pt(II) complexes

Nucleobases often act as polydentate ligands [17], coordinating either the same metal centre as chelate ligands, (see Pt(IV) complexes of Section 3.2.) or different

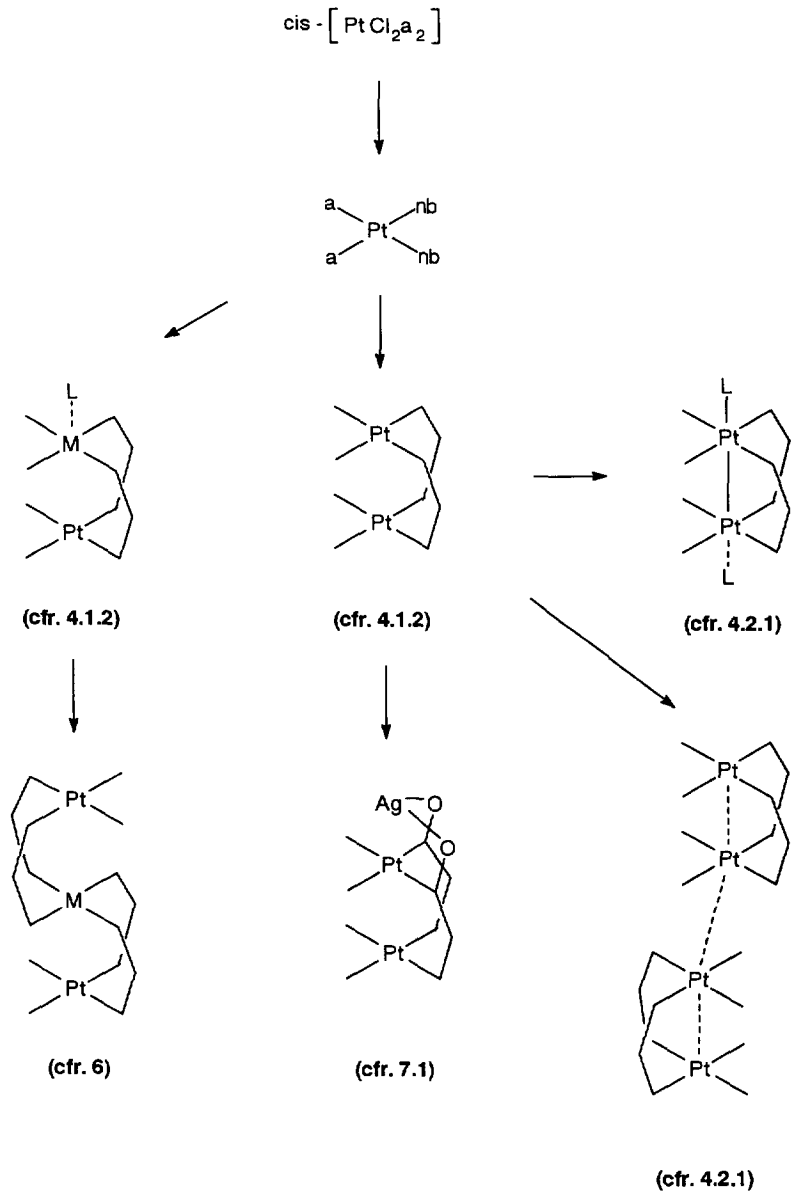

Fig. 5. Concise scheme of bi- and polynuclear species derived from *cis*-[(pym)$_2$Pta$_2$]. The numbers in parentheses refer to the section where the complex is discussed.

metal centres, as bridging ligands. Among the structurally characterized dinuclear species, examples with pym nucleobase complexes dominate. Concise schemes of bi- and polynuclear species obtained from *cis*- and *trans*-[(pym)$_2$Pta$_2$] complexes are sketched in Figs. 5 and 6, respectively. These figures also indicate where each type of the structurally characterized compound is described and discussed.

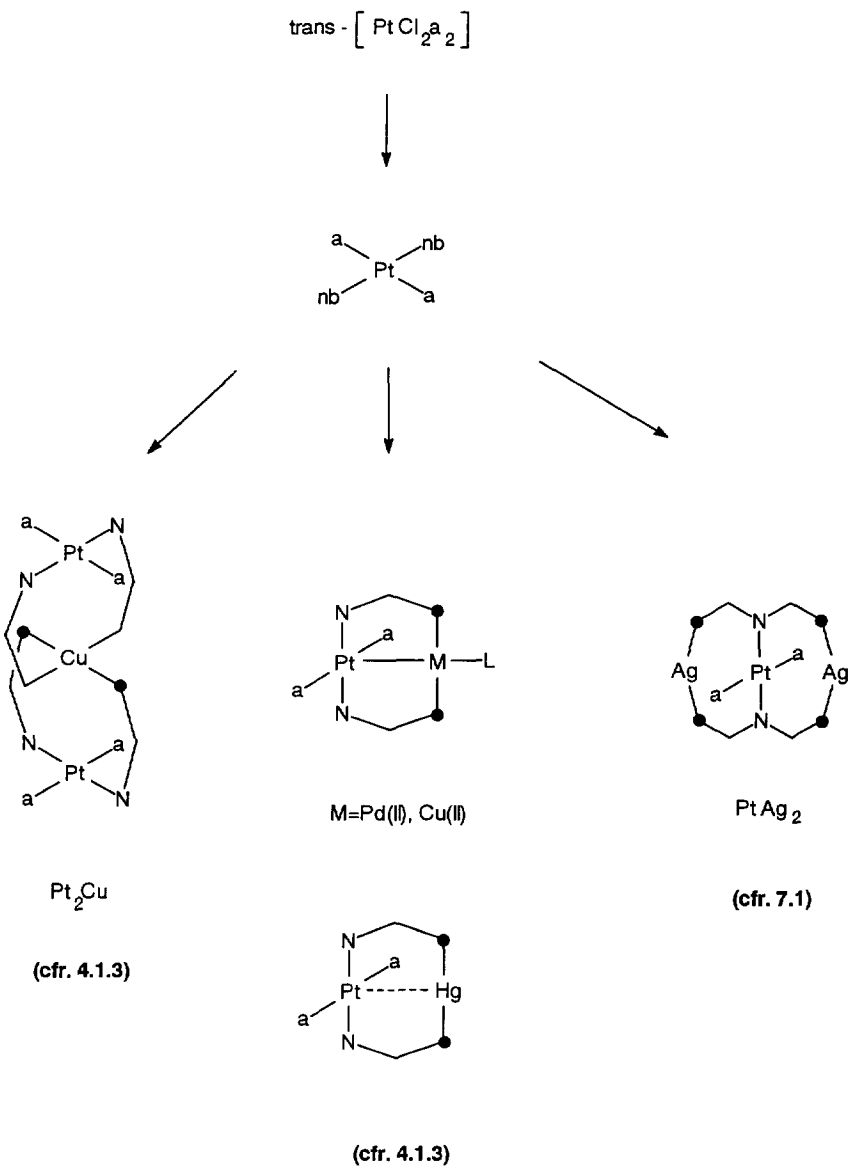

Fig. 6. Concise scheme of species derived from *trans*-[(pym)$_2$Pta$_2$]. The numbers in parentheses refer to the section where the complex is discussed.

4.1.1. Purine derivatives

The reported derivatives include a few examples with the deprotonated 9-methylguanine bridging two PtL_3 units (where L_3 is dien or L is NH_3) [87], and with the 9-methyladenine binding two $PtCl(NH_2Me)_2$ [78] or two $PtCl_2[S(O)(i\text{-}Pr)_2]$ units [88]. In each complex, Pt has a square-planar coordination

Table 4
Complexes with di- and trifunctional purine ligand

	Refcode	Pt1–N1	Pt2–N7	Pt3–N3	*d*1	*d*2	α1	α2	Ref.
Dinuclear									
[(dien)Pt(9-MeG$^-$,N^1,N^7)Pt(dien)]$^{3+}$	VERDUR	2.056	2.015	–	0.041	0.056	65.9	41.4	[87]
[(NH$_3$)$_2$(1-MeU$^-$,N^3)Pt(9-MeG$^-$,N^1,N^7)Pt(dien)]$^{2+}$	VERFAZ	2.038	2.018	–	0.006	0.053	69.6	61.7	[87]
[(iPr$_2$(O)S)Cl$_2$Pt(9-MeA,N^1,N^7)Pt(S(O)iPr$_2$)Cl$_2$]	*MAPSXP	2.08	2.07	–			89.0	61.0	[88]
Trinuclear									
trans-[(NH$_2$Me)$_2$ClPt(9-MeA,N^1,N^7)Pt(NH$_2$Me)$_2$Cl]$^{2+}$	LEBSAM	2.004	2.040	–	0.029	0.016	87.7	83.7	[78]
[(NH$_3$)$_3$Pt(9-MeA,N^1,N^7) Pt(NH$_3$)$_2$(9-MeA,N^7,N^1) Pt(NH$_3$)$_3$]$^{6+}$[a]	WAGTIH	2.029	1.978	–	0.000	0.026	89.9	89.4	[147]
[(9-EtG$^-$,N^1,N^3,N^7)(Pt(NH$_3$)$_3$)$_3$]$^{5+}$	DASCUV	2.034	2.045	2.032	0.038 0.011(*d*3)	0.061	83.4 64.8(*d*3)	80.8	[148]

[a] The central Pt located on a mirror plane.

geometry, and binding occurs via N1 and N7 of the purine bases. Scheme 1 sketches the purine backbone bridging two PtL_3 units through N1 and N7. Selected geometrical parameters of these complexes are reported in Table 4.

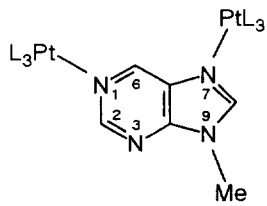

I

4.1.2. cis-(pym)$_2$Pta$_2$ derivatives

No example of a dinuclear complex containing a single pyrimidine bridge has been reported as yet, whereas a series of doubly bridged complexes has been structurally characterized either with h-h or h-t arrangement of the bases. The general composition is *cis*-$[a_2Pt(pym)_2MY_n]^{m+}$, where $m=2$, 1, 0, $n=2$, 3, and M is Pt^{2+}, Pd^{2+}, Cu^{2+}, Zn^{2+}, Ag^{+}. The bridging nucleobases are generally deprotonated.

When dinuclear complexes are prepared through a condensation reaction between mononuclear complexes

$$2[(NH_3)_2Pt(pym)H_2O]^{+} \xrightarrow{-H_2O} [(NH_3)_2Pt(pym)_2Pt(NH_3)_2]^{2+}$$

usually h-t dinuclear species are obtained, as sketched in Fig. 7, **II**. Another way to obtain dinuclear complexes is the condensation of a neutral *cis*-$[(pym)_2Pt(NH_3)_2]$ complex with cations of type *cis*-$[a_2M(H_2O)_2]^{2+}$ where a is NH_3, a_2 is en, bipy, and M is Pt, Pd or $[M(H_2O)_n]^{m+}$ or with the $[Pt(NH_3)Cl_3]^{-}$ and $[PtCl_4]^{2-}$ anions. In this case the reaction gives h-h species (Fig. 7, **III**) [89].

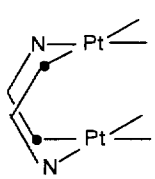

II

h-t

4:4 (M=Pt,Pd)

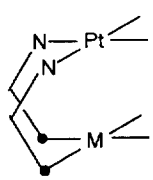

III

h-h

4:4 (M=Pt,Pd)

4:5 (M=Zn, Cu)

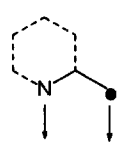

Fig. 7. Head–head (h-h) and head–tail (h-t) configurations in cis dinuclear species with difunctional nucleobases. The symbolism *n:m* indicates the number of ligands about Pt and M, respectively.

Table 5
Dinuclear complexes

	Refcode	Pt...M	Pt–N3 Pt–N3 Pt–a Pt–a	M–O4 M–O4 M–Y M–Y	*d*1 *d*2	β	τ	ω	Ref.
h-h cis-$[a_2Pt(II)(pym)_2MY_2]^{m+}$									
$[(NH_3)_2Pt(1\text{-}MeT^-,N^3,O^4)_2Pt(NH_3)_2]^{2+}$	MTAPTN10	2.926	2.032 2.043 2.060 2.046	2.011 2.024 2.031 2.036	0.050 0.077	85.7	31.4	2.3	[93]
$[(NH_3)_2Pt(1\text{-}MeT^-,N^3,O^4)_2PtCl(NH_3)]^{1+}$	SIBTIG	2.938	2.049 2.044 2.049 2.059	2.010 2.041 2.278 2.056	0.067 0.096	84.9	31.5	1.8	[89]
$[(NH_3)_2Pt(1\text{-}MeT^-,N^3,O^4)_2PtCl_2]^0$	SIBTOM	2.861	2.026 2.025 2.063 2.055	2.030 2.009 2.271 2.277	0.022 0.051	89.1	22.5	2.4	[89]
$[(NH_3)_2Pt(1\text{-}MeU^-,N^3,O^4)_2Pt(NH_3)_2]^{2+}$	BULWAG	2.937	2.051 2.045 2.015 2.078	2.040 2.024 2.013 2.005	0.063 0.081	84.7	34.1	21.9	[94]
$[(NH_3)_2Pt(1\text{-}MeU^-,N^3,O^4)_2Pt(bipy)]^{2+}$	SIDPEA	2.929	2.058 2.046 2.062 2.070	2.014 2.048 2.005 1.985	0.024 0.081	83.1	30.4	12.8	[95]
$[(NH_3)_2Pt(1\text{-}MeC,N^3,O^2)(1\text{-}MeU^-,N^3,O^4)$ $Ag(I)(ONO_2)(H_2O)]^{1+}$	FATBIL	2.907	2.047 2.034 2.069 2.038	2.470[b] 2.352 2.458 2.521	0.007 0.660	75.9	33.5	–	[91]
$[(NH_3)_2Pt(1\text{-}MeU^-,N^3,O^4)_2Pd(II)(en)]^{2+}$	GAWTIH	2.927	2.044 2.039 2.040 2.036	2.039 2.046 2.015 2.028	0.039 0.099	83.6	34.2	17.3	[96]
$[(NH_3)_2Pt(1\text{-}MeU^-,N^3,O^4)_2Cu(II)(H_2O)_2]^{2+}$	BOSSUX	2.765	1.994 1.997 2.032 2.002	1.926 1.969 1.964 2.035	0.039 0.073	89.4	25.7	12.7	[54]

$[(NH_3)_2Pt(1\text{-}MeC^-,N^3,O^4)_2Zn(H)(H_2O)_3]$	DIGJAL	2.760	2.050 2.052 2.042 2.043	2.090 2.036 2.111 2.088	0.042 0.139	85.7	19.5	17.4	[97]
	Refcode	Pt…Pt	Pt1–N3 Pt1–X4[c] Pt1–a Pt1–a	Pt2–X4[c] Pt2–N3 Pt2–a Pt2–a	*d*1 *d*2	β	τ	ω	Ref.
h-t cis-[a₂Pt(II)(pym)₂Pt(II)a₂]$^{m+}$									
$[(NH_3)_2Pt(1\text{-}MeC^-,N^3,N^4)_2Pt(NH_3)_2]^{2+}$	MCTPTA	2.981	2.043 2.064 2.054 2.101	2.008 2.059 2.028 2.065	0.032 0.043	77.3	34.2	15.8	[98]
$[(NH_3)_2Pt(1\text{-}MeT^-,N^3,O^4)_2Pt(NH_3)_2]^{2+}$	BONZOT	2.915	2.075 2.007 2.027 2.105	2.039 2.014 2.008 2.044	0.058 0.094	80.5	30.7	18.6	[99]
	BONZOT	2.923	2.086 2.060 2.046 2.076	2.011 2.046 2.074 2.043	0.058 0.056	70.5	35.2	24.4	
$[(NH_3)_2Pt(1\text{-}MeT^-,N^3,O^4)_2Pt(NH_3)_2]^{2+}$	MTHYAP	2.974	2.064 2.013 2.053 2.092	2.037 2.013 2.050 2.053	0.115 0.040	86.0	36.8	13.4	[100]
$[(NH_3)_2Pt(1\text{-}MeU^-,N^3,O^4)_2Pt(NH_3)_2]^{2+}$	MURCPT	2.953	2.048 2.067 2.052 2.076	2.031 2.051 2.045 2.040	0.065 0.046	73.2	35.9	18.9	[101]
$[(PMe_3)_2Pt(1\text{-}MeC^-,N^3,N^4)_2Pt(PMe_3)_2]^{2+}$	VIDWAG	3.199	2.119 2.058 2.260 2.264	2.074 2.108 2.258 2.263	0.186 0.176	80.2	46.5	8.2	[102]
$[(bmik)Pt(1\text{-}MeT^-,N^3,O^4)_2Pt(bmik)]^{2+}$	*	2.900	2.015 2.009 1.963 1.988	2.007 2.040 1.959 2.024			11.0	23.0	[51]
$[(bmik)Pt(1\text{-}MeU^-,N^3,O^4)_2Pt(bmik)]^{2+}$	*	2.841	2.033 2.038 2.005 1.982	2.038 2.033 1.982 2.005	0.08 0.08		25.0	25.0	[51]

[a] Additional X ligand in Pt-Cu and Pt-Zn derivatives. [b] M–O2 distance. [c] X4 = O4 for pym = 1-MeT$^-$ or 1-MeU$^-$, = N4 for 1-MeC$^-$.

The uracilate and thyminate anions simultaneously bind the metals through N3 and the carbonyl oxygen O4, whereas the 1-methylcytosine anions do so through N3 and the deprotonated amino group N4. The neutral cytosine was also found to act as a bridging ligand through N3 and O2 (see below).

Following the notation introduced by Balch [90] the symbolism 4:4, reported in Fig. 7, indicates the number of ligands around Pt and M, respectively. The notation 4:5 refers to species where M is Zn^{2+} or Cu^{2+}, because of an additional axial ligand about these metals.

For steric reasons, the metal coordination planes are not parallel but slightly tilted (see below).

According to the syntheses described above, the *cis*-diplatinum(II) complexes have been found to have either the geometry **II** or **III**, while the heterobimetallic ones have only the geometry **III**, with Pt coordinated to the endocyclic pyrimidine N atom. It is of interest to note that in the Pt,Ag compound h-h *cis*-$[(NH_3)_2Pt(1\text{-}MeC,N^3,O^2)(1\text{-}MeU^-,N^3,O^4)Ag(ONO_2)(H_2O)]^+$ two different nucleobases, one of which is a neutral cytosine coordinating through N3 and O2, bridge the metal centres [91]. A similar situation is envisaged in a Pt_2Cu heteronuclear complex [92] (see also Section 5).

Some geometrical parameters for the Pt(II),M complexes are given in Table 5, i.e. the Pt–M distance, the metal coordination bond lengths, the displacements of Pt ($d1$) and M ($d2$) out of their respective coordination planes, the dihedral angles, β, between the two nucleobases and, τ, between the Pt and M coordination planes, and the average torsion angle ω about the Pt–M vector.

Pt–Pt distances vary from 2.861 Å in h-h *cis*-$[(NH_3)_2Pt(1\text{-}MeT^-,N^3,O^4)_2PtCl_2]$ to 3.199 Å in h-t *cis*-$[(PMe_3)_2Pt(1\text{-}MeC^-,N^3,N^4)_2Pt(PMe_3)_2]^{2+}$. Correspondingly, in the above complexes, the angles τ vary from 22.5 to 46.5°.

Recently, two dinuclear cations *cis*-$[(bmik)Pt(pym)_2Pt(bmik)]^{2+}$ (where pym is 1-MeT$^-$ and 1-MeU$^-$) have been synthetized, containing the bis(*N*-methylimidazol-2-yl)ketone (bmik) ligand [51]. The Pt–Pt distance of 2.841 Å, is the shortest so far reported for 1-methyluracilate complexes. The dihedral angle between the coordination planes is 25° (11° in the cation with 1-MeT$^-$), in contrast to a range of 30–37° found in the amino derivatives, while the coordination planes are rotated about the Pt·Pt vector by approx. 24°.

In heterobimetallic complexes the Pt–M distances are in the range found for diplatinum species when M is Pd^{2+} (2.927 Å), or Ag^+ (2.907 Å), whereas they are significantly shorter when M is Cu^{2+} (2.765 Å) or Zn^{2+} (2.760 Å).

The fair linear relationship ($r=0.92$) between Pt–M and the angle τ for 14 dinuclear complexes (Fig. 8) suggests that the increase in Pt–M and τ is to be attributed mainly to the steric repulsion between the Pta_2 and MY_2 moieties, which increases with the increasing ionic radius of M and with the bulk of ligands a_2 and Y_2. This effect may be modulated in some cases by a tilt of coordination planes about the Pt–M vector. However, as suggested by the above mentioned Pt–bmik derivatives, stacking interaction among these ligands also facilitates a close approach of the metal coordination planes in the dinuclear complex.

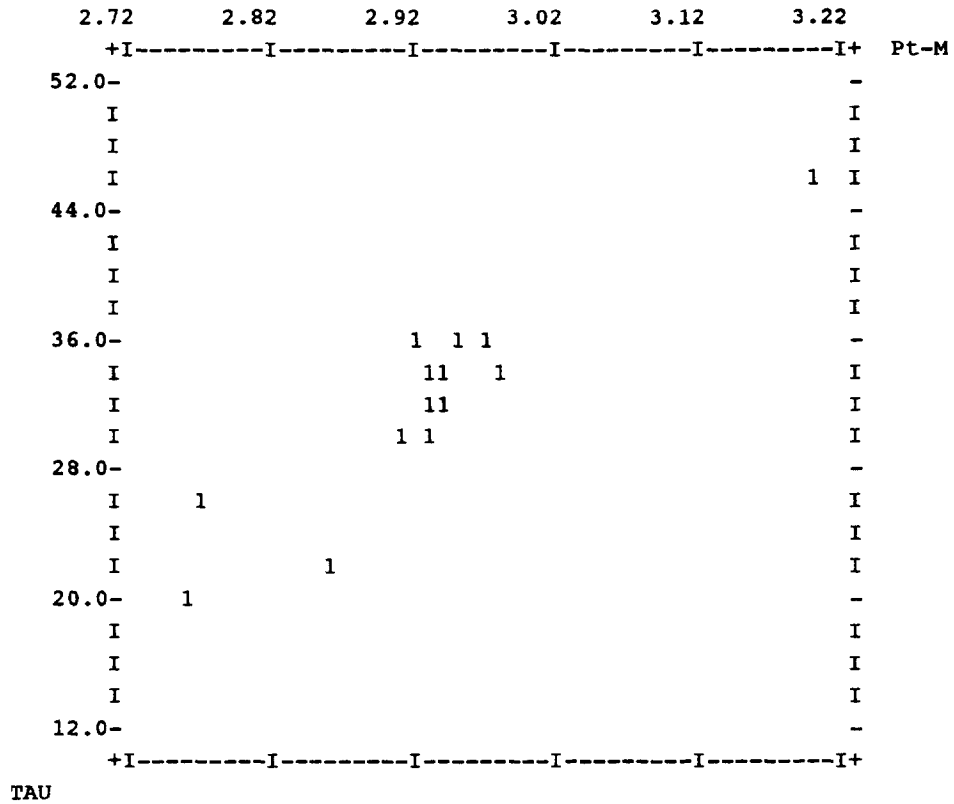

Fig. 8. Plot of Pt–M distances *vs.* the dihedral angle between the metal coordination planes in *cis*-$[a_2Pt(pym)_2MY_n]^{m+}$ complexes.

The Pt–N3 bond lengths (mean value 2.041 Å, $n=28$, excluding the phosphine derivative VIDWAG) do not differ from those found in mononuclear species, suggesting that this distance is not influenced significantly when pyrimidine acts as bidentate ligand.

The dinuclear h-h Pt,M units have been found to pack in the solid state in three different patterns [17]: (i) centrosymmetric arrangements of type (Pt,M).(M,Pt) with M next to each other as detected in BOSSUX, BEKKOR, and FOCHEK or (ii) (M,Pt).(Pt,M) with Pt atoms next to each other as found in BULWAG; (iii) (Pt,M) units subsequently arranged in a staircase fashion as, for example, in MTAPTN10.

4.1.3. trans-(pym)$_2$Pta$_2$ derivatives

A dinuclear trans species of type **IV** (Fig. 9) has never been isolated, possibly as a consequence of an unfavourable steric interaction between the amine ligands at the two adjacent metals, which prevents its formation. This was suggested

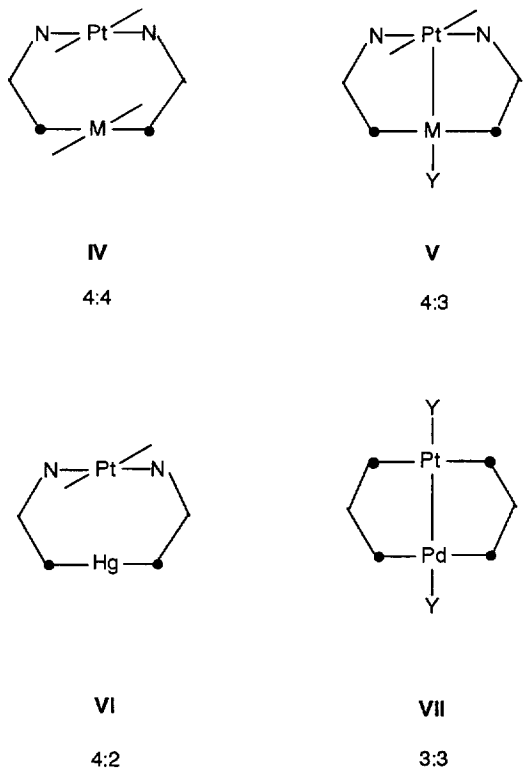

Fig. 9. *Trans*-dinuclear species 4:4, 4:3, and 4:2 with h-h arrangement of nucleobases. Fragment VII represents dinuclear Pt(I)–Pd(I) species.

by a trans→cis isomerization observed during the reaction of *trans*-$[(1\text{-MeC},N^3)_2Pd(NH_3)_2]^{2+}$ with *trans*-$[(NH_3)_2Pd(H_2O)_2]^{2+}$ to give the h-t cis dipalladium species of type **II** [103].

However, more recently [104–106], several examples of heterobimetallic complexes with a trans h-h arrangement of the bridging 1-MeC^- monoanions have been obtained. These complexes of general formula *trans*-$[a_2Pt(1\text{-}MeC^-,N^3,N^4)_2MY]^{n+}$, (M is Pd^{2+}, Cu^{2+}, a is NH_3 or NH_2Me), (Fig. 9, **V**) are characterized by Pt–M distances, which are very short compared with those found in **II** and **III**, and by two approximately coplanar 1-MeC^- ligands. Any possible steric clash between the amines at Pt(II) and ligands at M is avoided in these arrangements. In fact there are no ligands at M that are parallel to the amine ligands at Pt. Extending this investigation to species where M is a d^{10} metal ion, analogous complexes of formula *trans*-$[a_2Pt(1\text{-}MeC^-,N^3,N^4)_2Hg]^{2+}$ have also been reported [107] (Fig. 9, **VI**). An ORTEP drawing of *trans*-$[(MeNH_2)_2Pt(1,5\text{-}Me_2C^-,N^3,N^4)_2Hg]^{2+}$ is depicted in Fig. 10. Selected geometrical data for the complexes so far structurally characterized are reported in Table 6.

Table 6
Dinuclear complexes h-h *trans*-$[a_2Pt(II)(1\text{-}MeC^-,N^3,N^4)_2MY]^{m+}$

	Refcode	Pt–M	Pt–N3 Pt–N3 Pt–a Pt–a	M–N4 M–N4 M–Y	d(Pt) d(M)	β	τ	Ref.
$[(NH_3)_2Pt(1\text{-}MeC^-,N^3,N^4)_2Pd(NH_3)]^{2+}$	TALVEH	2.511	2.011 2.024 2.040 2.034	2.005 2.014 2.001	0.032 0.029	8.0	88.4	[104,105]
$[(NH_3)_2Pt(1\text{-}MeC^-N^3,N^4)_2PdCl]^{1+}$	TALVIL	2.518	2.005 2.021 2.017 2.022	1.989 1.980 2.314	0.009 0.061	4.4	81.6	[104,105]
$[(NH_3)_2Pt(1\text{-}MeC^-,N^3,N^4)_2Pd(1\text{-}MeU^-,N^3)]^{1+}$	TALVOR	2.515	2.021 2.020 2.021 2.036	1.985 1.994 2.055	0.013 0.009	5.0	87.3	[104,105]
$[(NH_2Me)_2Pt(1\text{-}MeC^-,N^3,N^4)_2Pd]_2(pyz)^{4+}$ (pyrazine bridges two Pt,Pd units)	SUJLIS	2.492	2.071 2.046 2.029 1.964	1.993 1.996 2.042	0.025 0.024	5.7	88.2	[105]
$[(NH_2Me)_2Pt(1\text{-}MeC^-,N^3,N^4)_2Pd(SCN)]^{1+}$	SUJLOY	2.521	2.019 2.028 2.047 2.043	1.983 2.018 2.288	0.022 0.011	2.9	89.4	[105]
$[(NH_2Me)_2Pt(1\text{-}MeC^-,N^3,N^4)_2Hg]^{2+}$	PEJYAE	2.785	2.037 2.035 2.091 2.053	2.040 2.003 [a]	0.016	6.1		[107]
$[(NH_2Me)_2Pt(1,5\text{-}Me_2C^-,N^3,N^4)_2Hg]^{2+}$	PEJYIM	2.764	2.054 2.019 2.055 2.040	2.033 2.036 [a]	0.012	7.0	–	[107]
$[(NH_2Me)_2Pt(1\text{-}MeC^-,N^3,N^4)_2Hg]^{2+}$	PEJYEY	2.835	2.035 2.035 2.034 2.033	2.116 2.116 [a]	0.020	7.6	–	[107]
$[(NH_2Me)_2Pt(1\text{-}MeC^-,N^3,N^4)_2Cu]_2(CO_3)^{2+}$ (CO_3 bridges two Pt,Cu units)	*	2.495 2.505						[106]
$[(NH_2Me)_2Pt(1\text{-}MeC^-,N^3,N^4)_2Cu(NH_3)(H_2O)]^{2+}$	*	2.557						[106]
$[(NH_2Me)_2Pt(1\text{-}MeC^-,N^3,N^4)_2Cu(9\text{-}EtGH,N^7)]^{2+}$	*	2.500						[106]

[a] Hg has additional contacts with NO_3^- and Cl^- in the range 2.67–2.77 Å.

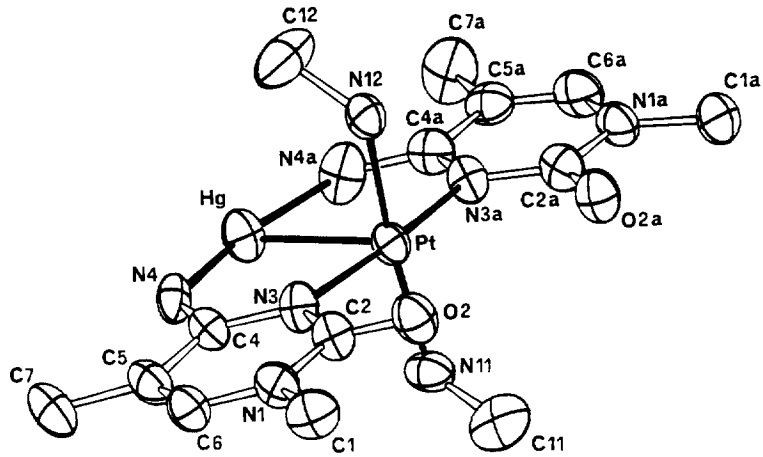

Fig. 10. ORTEP drawing of dinuclear cation *trans*-$[(MeNH_2)_2Pt((1,5\text{-}Me_2C^-,N^3,N^4)_2Hg]^{2+}$ (PEJYIM).

In the 4:3 heterobimetallic complexes derived from *trans*-$[(pym)_2Pta_2]$ the coordination planes of Pt and Pd (or Cu) are approximately perpendicular to each other, and the interplanar angles between the two cytosinate planes range from 3.7 to 7.1°, with the two trans bases in a h-h arrangement [105,106]. No significant change in the Pt–N3(cytosine) distances with respect to those found in cis dinuclear species **II** and **III** have been evidentiated.

The Pt–Pd distances of about 2.50 Å are among the shortest reported so far, even shorter than those found in Pt(I)–Pd(I) dinuclear species (mean value 2.558 Å) with different bridging ligands [108], having the geometry shown in Fig. 9, **VII**.

A further comparison of the Pt–M bond lengths with those of 4:4 cis complexes shows that in the latter, the Pt–Pd distances are lengthened by about 0.40 Å, and the Pt–Cu distances by about 0.25 Å.

The Pt–Pd distance does not appear to be significantly influenced upon variation of the ligand Y in the series *trans*-$[a_2Pt(1\text{-}MeC^-)_2PdY]^{n+}$ (Fig. 9, **V**), in contrast to ^{195}Pt NMR chemical shifts, that span a range of 500 ppm. The variation of ^{195}Pt chemical shifts display a linear dependence with electronegativity of halide, while no simple relationship is evident with the nature of Y ligands other than halides [105].

The complex *trans*-$[a_2Pt(1\text{-}MeC^-)_2PdCl]NO_3$ has been used to study the binding properties of palladium(II) with various derivatives of aminoacids mimicking the side-chain metal binding sites of proteins [109].

The Pt–Hg intermetallic distances (around 2.80 Å) are shorter than the mean values of the Pt–Pt and Hg–Hg distances measured in homodinuclear h-t *cis*-$[(NH_3)_2Pt(1\text{-}MeC^-,N^3,N^4)_2Pt(NH_3)_2]^{2+}$ [98], and $[(MeHg)_2(1\text{-}MeC^-,N^3,N^4)_2]^+$, [110] respectively. The distance of 2.80 Å is at the upper limit of Pt–Hg distances in the range reported by van Koten et al. [111], who stated that this distance is indicative of a weak bonding interaction.

Table 7
Dinuclear complexes

	Refcode	Pt–Pt	Pt1–N3 Pt1–N3 Pt1–a Pt1–a Pt1–X	Pt2–O4 Pt2–O4 Pt2–Y Pt2–Y Pt2–Y	*d*1 *d*2	*β*	*τ*	*ω*	Ref.
h-h cis-[a$_2$*XPt(III)(pym)*$_2$*Pt(III)Y*$_3$*]*$^{m+}$ [a]									
$[(NH_3)_2Pt(1\text{-}MeU^-,N^3,O^4)_2Pt(NH_3)_2(NO_2)]^{3+}$	DIRGEQ	2.606	2.017 2.021 2.065 2.068 –	2.039 2.011 2.033 2.031 2.058	0.078 0.056	79.7	19.1	3.2	[115]
$[(NH_3)_2Pt(1\text{-}MeU^-,N^3,O^4)_2Pt(NH_3)_2(1\text{-}MeU^-,C^5)]^{3+}$ (1-MeU$^-$, *C5 deprotonated*)	DIPTOL	2.684	2.013 2.027 2.044 2.039 –	1.985 2.007 2.040 2.043 2.037	0.104 0.066	86.9	23.2	6.4	[116]
$[(NH_3)_2ClPt(1\text{-}MeU^-,N^3,O^4)_2Pt(NH_3)_2Cl]^{2+}$	DOKJIW	2.572	1.864 2.053 2.049 2.049 2.459	2.016 2.001 2.020 2.039 2.426	0.012 0.062	65.1	20.3	23.5	[117]
$[(NH_3)_2ClPt(1\text{-}MeU^-,N^3,O^4)_2PtCl_3]^0$	DOKJOC	2.543	2.051 2.056 2.049 2.039 2.465	2.029 2.022 2.295 2.285 2.417	0.058 0.010	69.9	16.0	29.8	[117]
$[(NH_3)_2(NO_2)Pt(1\text{-}MeC^-,N^3,N^4)_2Pt(NH_3)_2(NO_2)]^{2+}$	MCTPTB	2.584	2.001 2.003 2.061 2.051 2.121	2.015[b] 2.062[b] 2.081 2.067 2.126	0.036 0.011	77.2	20.6	25.2	[98]
$[(NH_3)_2(H_2O)Pt(1\text{-}MeT^-,N^3,O^4)_2PtCl_3]^{1+}$ (disordered ligands)	SEMGAS	2.556							[118]

$[(NH_3)_2Pt(2.25)(1\text{-}MeU^-,N^3,O^4)_2Pt(2.25)(NH_3)_2]_2^{5+}$			Pt1	Pt2					
(tetranuclear cation)	COPPOM10	2.810	2.026	2.009	0.072	89.4	27.3	6.2	[119]
			2.024	2.021	0.067				
			2.076	2.015					
			2.012	2.003					
			Pt4	Pt3					
	COPPOM10	2.793	2.025	2.023	0.077	84.8	26.4	8.4	
			2.078	2.035	0.056				
			2.036	2.049					
			2.056	2.037					
$[(NH_3)_2Pt(2.75)(1\text{-}MeT^-,N^3,O^4)_2Pt(2.75)Cl_2]_2Cl^{2+}$	SEMGEW	2.699	2.033	2.035	0.019	85.8	20.6	21.8	[118]
(Cl bridges two Pt,Pt units)			2.027	2.051	0.031				
			2.058	2.288					
			2.046	2.283					

	Refcode	Pt–Pt	Pt1–N3 Pt1–O4 Pt1–a Pt1–a Pt1–X	Pt2–O4 Pt2–N3 Pt2–a Pt2–a Pt2–Y	*d*1 *d*2	β	τ	ω	Ref.
h-t cis-$[a_2XPt(III)(pym)_2Pt(III)a_2Y]^{m+}$									
$[(NH_3)_2(H_2O)Pt(1\text{-}MeU^-,N^3,O^4)_2Pt(NH_3)_2(NO_2)]^{3+}$	CASDAB	2.574	2.051	2.016	0.046	83.8	21.5	29.0	[120]
			2.017	2.054	0.029				
			2.013	2.057					
			2.065	2.048					
			2.253	2.080					
$[(NH_3)_2(H_2O)Pt(1\text{-}MeU^-,N^3,O^4)_2Pt(NH_3)_2(ONO_2)]^{3+}$	DUXBED	2.556	2.040	2.016	0.056	75.4	22.6	29.4	[121]
			1.998	2.046	0.050				
			2.055	2.017					
			2.030	2.067					
			2.176	2.142					
$[(NH_3)_2(H_2O)Pt(1\text{-}MeU^-,N^3,O^4)_2Pt(NH_3)_2(ONO_2)]^{3+}$	DUXBIH	2.560	2.048	2.035	0.042	77.2	22.7	28.7	[121]
			2.037	2.022	0.056				
			2.056	2.016					
			2.054	2.032					
			2.172	2.120					

[a] Different oxidation states from +3 indicated in the formula. [b] N4 of $1\text{-}MeC^-$.

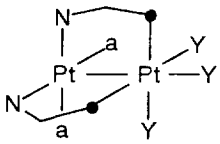

VIII

4:5 h-h

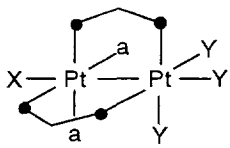

IX

5:5 h-h or h-t

4.2. *Pt in oxidation state > 2*

4.2.1. *Pyrimidine bases*

The interest in diplatinum(III) complexes [112] containing pyrimidine nucleobases as bridging ligands relates to their possible role as components of a class of anticancer agents, the so called *platinum pyrimidine blues* and their role as likely intermediates leading to the formation of the blues [113,114].

They are prepared from diplatinum(II) complexes through treatment with a variety of oxidizing agents.

Dinuclear species of kind *cis*-$[a_2X_nPt(pym)_2PtY_3]^{m+}$ as sketched in **VIII** ($n=0$) and **IX** ($n=1$), usually have Pt in +3 oxidation state. They are reported in Table 7 together with geometrical parameters as those given in Table 5.

From a structural point of view these dinuclear complexes are very similar to the Pt(II) dimers of type **II** and **III**, previously described, with a cis configuration of the bridged nucleobases about the metal centers but with an additional axial ligand coordinated to one or both Pt centers. The three complexes of kind **VIII** have a h-h arrangement of the nucleobases, whereas those of kind **IX** exhibit both h-h and h-t configurations.

Using the notation introduced by Balch [90], and already applied to the binuclear species of Section 4.1, they can be classified into 4:5 and 5:5 species. For the former an alternative description implies a Pt(II)–Pt(IV) dimetallic core.

An exception to the +3 oxidation state of Pt is realized in a tetranuclear cation (SEMGEW) where a Cl bridges two Pt dimers (**X**) with metals in a mean +2.75 oxidation state [118].

A previously reported 1-MeC$^-$ compound (MCTPTB, Table 7), then interpreted as a Pt(2.5) compound of composition *cis*-$[(NH_3)_2(NO_2)Pt(1\text{-}MeC^-,N^3,N^4)_2Pt(NH_3)(NO_2)](NO_3)_2\cdot H_5O_2^+$, in fact is a diplatinum(III) compound containing $2H_2O$ instead of a $H_5O_2^+$ [98]. Its Pt–Pt distance of 2.584 Å is well within the range of most of the other structurally similar diplatinum(III) compounds listed in Table 7.

With respect to the 4:4 Pt(II) complexes, the increase in oxidation number of Pt to +3 causes a significant decrease in metal–metal distances, which now range from

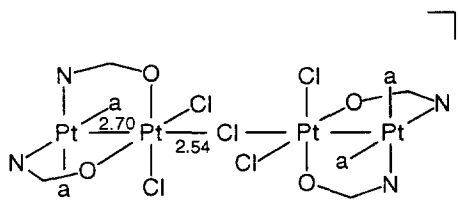

X

2.543 to 2.699 Å. The 4:5 species appear to exhibit distances slightly longer than those in 5:5 ones.

An appreciable lengthening of the Pt–Pt distance is apparent when a strong trans influencing axial ligand Y_{ax}, collinear with the two metals, is present [116]. In the fragment X_{ax}-Pt–Pt–Y_{ax} (**IX**), the trans influence of Y_{ax} is transmitted to the metal–metal bond, which in turn exerts a strong trans influence, lengthening the Pt–X_{ax} bond to an extent that leads to formation of the 4:5 species (**VIII**). In fact, in the latter Y_{ax} is either a NO_2, [115] or a σ–bonded C atom of a nucleobase, C(5) of 1-MeU$^-$ [116]. The fact that Pt bonded to Pt exerts an appreciable trans influence is suggested in 5:5 species where the Pt–Y_{ax} distances are substancially longer than the Pt–Y_{eq} ones. Thus, for example, in *cis*-[Cl$(NH_3)_2$Pt(1-MeU$^-$,N^3,O^4)$_2$PtCl$_3$] the two axial Pt–Cl distances are 2.465 and 2.417 Å, whereas the equatorial ones are 2.285 and 2.295 Å [117].

The angles between the Pt coordination planes in these diplatinum(III) compounds, which are in the range 16°–23°, are smaller than those found in the cis diplatinum(II) analogues (22–46°). This is a consequence of the Pt–Pt bonding interaction in the former. The relief of steric interaction between the Pt moieties in the Pt(III)–Pt(III) complexes generally occurs through an increase of the torsional angles, ω, (mean value 22.3(3)°) with respect to those of the Pt(II) analogues (mean 13(2)°). The angle between the two bridging nucleobases fall in the range 65°–87°, similar to that observed in the dinuclear cis complexes (Table 5).

No significant difference can be detected (within the experimental errors) between the Pt–nb distances in the present complexes and those in the cis diplatinum(II) analogues. Lippard et al. reported mixed valence Pt_4 chain complexes containing pyridone or 1-MeU$^-$ bridging ligand [119]. The structures are built up of two binuclear units associated via H bonding and partial metal–metal bond formation. The scheme **XI** depicts the tetranuclear species *cis*-[$(NH_3)_2$Pt-(1-MeU$^-$,N^3,O^4)$_2$Pt$(NH_3)_2$]$_2^{5+}$ (COPPOM10), which has a zigzag arrangement characterized by an outer pair of Pt–Pt bonds [2.810 and 2.793 Å], which is shorter than the inner one [2.865 Å]. The mean metal oxidation state is +2.25, but formally the tetranuclear platinum blue contains one Pt(III) and three Pt(II), with the unpaired electron located in a dz^2-derived MO delocalized over the four Pt atoms.

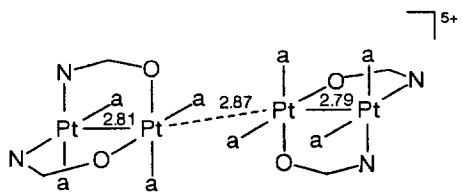

XI

4.2.2. S-containing bases

Structurally related diplatinum(III) complexes containing S ligands such as pyrimidine-2-thione ($pymS^-$) or 2-thiouracilato (TU^-) have been reported by Goodgame and coworkers [122–124]. Pt binding in these "lantern-type" complexes [125], of composition $[XPtL_4PtX]^0$, is via N and the adjacent S of the L ligand. The terminal axial position, usually occupied by halide anions X^-, can be replaced also by a monodentate $pymS^-$ bonded through sulphur. Of the four possible mutual orientations of the bridging ligands, only the h-h-h-t (**XII**) and h-h-t-t (**XIII**) are found in these complexes. The Pt–Pt distances, reported in Table 8, are close to those reported for dinuclear Pt(III) complexes (see previous Section), but dihedral angles between the metal coordination planes are close to zero, leading to nearly parallel planes. The values of the Pt–Cl axial bond distances, which are in the range 2.44–2.46 Å, again confirm the high trans influence of the Pt–Pt bond.

5. Trinuclear complexes

Most of the trinuclear complexes so far reported are of composition *cis*-$[a_2Pt(II)(pym)_2M(pym)_2Pt(II)a_2]^{m+}$, with M is Cu^{2+}, Mn^{2+}, Pd^{2+}, Pd^{3+}, Ag^+,

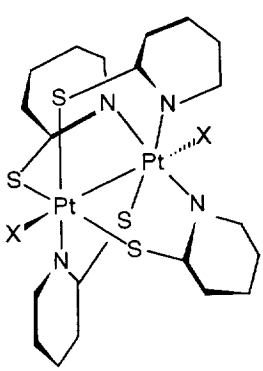

XII

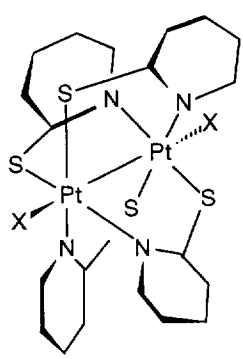

XIII

Table 8
Dinuclar $[XPt(III)L_4Pt(III)X]^0$ complexes with L = thioderivative

	Refcode	X–Pt1	Pt1–Pt2	Pt2–X	Pt1–L1 Pt1–L2 Pt1–L3 Pt1–L4	Pt2–L1 Pt2–L2 Pt2–L3 Pt2–L4	*d*1 *d*2	τ	ω	Ref.
h-h-h-t[ClPt(pymS$^-$,N^1,S)$_4$PtCl]^0	FAWJIW	2.463	2.517	2.440	2.060 N 2.099 N 2.295 S 2.056 N	2.347 S 2.305 S 2.122 N 2.339 S	0.020 0.031	1.1	15.1	[122]
h-h-t-t[IPt(TU$^-$,N^1,S)$_4$PtI]^0	FAWJOC	2.775	2.546	2.766	2.126 N 2.008 N 2.298 S 2.296 S	2.304 S 2.284 S 2.099 N 2.104 N	0.015 0.001	2.1	12.9	[122]
h-h-t-t[BrPt(pymS$^-$,N^1,S)$_4$Pt(pymS$^-$,S)]^0	FAWJUI	2.618	2.554	2.486	2.085 N 2.100 N 2.297 S 2.300 S	2.310 S 2.283 S 2.089 N 2.080 N	0.013 0.018	1.8	12.6	[122]
h-h-t-t[IPt(pymS$^-$,N^1,S)$_4$PtI]^0	*CUSHUT	2.768	2.554	2.779						[123]
h-h-t-t[ClPt(pymS$^-$,N^1,S)$_4$Pt(pymS$^-$,S)]^0	*JADYOC	2.494	2.547	2.438						[124]

Tl^+ and pym are deprotonated ligands. Pertinent structural data are given in Table 9. In principle, with square-planar metal centres the nucleobase bite allows for two possible arrangements, **XIV** and **XV** (Fig. 11), depending on whether the Pt ions adopt cis or trans configurations.

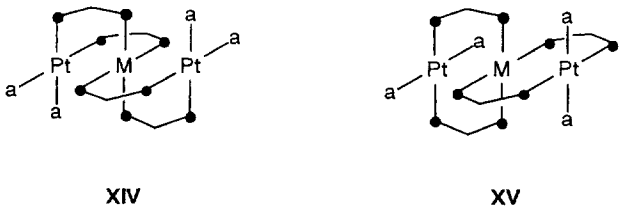

XIV **XV**

Fig. 11. Trinuclear complexes with cis (**XIV**) and trans (**XV**) configurations of the bridging bases.

The possible h-h or h-t arrangements of the two pairs of nucleobases imply the existence of many isomers of **XIV** and **XV**. However, since the cis trinuclear species are prepared starting from mononuclear *cis*-$[(pym,N3)_2Pta_2]$ complexes, only the isomer of type **XIV** has been obtained, where M is coordinated by the pyrimidine O donors (usually O4), with the bridging pym ligands in a h-h arrangement. Only in the compound $[(NH_3)_2Pt(1\text{-}MeC)(1\text{-}MeU^-)Cu(1\text{-}MeC)(1\text{-}MeU^-)Pt(NH_3)_2]^{2+}$, where the cytosines act as neutral ligands, Cu is coordinated through two O2 sites of 1-MeC and two O4 atoms of $1\text{-}MeU^-$ [92].

As found for dinuclear species *cis*-$[a_2Pt(pym)_2MY_n]^{m+}$, the geometry of **XIV** avoids any steric clash between facing ligands at Pt and M better, mainly through an outward tilting of the Pt coordination planes. In contrast, species of type **XV** are expected to be much more subject to restraints (see below).

There is an ambiguity in complexes containing $1\text{-}MeT^-$ as far as the differentiation of the two exocyclic oxygens are concerned. This is a consequence of the pseudo two-fold axis through N3 and C6 (see for example Ref. [128], where M is Mn). However, since O4 appears to be more basic than O2, primary coordination is expected to occur through O4, as it happens in $1\text{-}MeU^-$ derivatives.

In all the trinuclear cations but two (M is Ag^+ or Tl^+), M lies on a crystallographic symmetry center, so that the two Pt–M distances are equal and the MO_4 atoms are rigorously coplanar. On the contrary, in the case of M is Ag^+ and Tl^+, these metals have a distorted tetrahedral arrangement of the four O donors. The (Pt,Tl,Pt) structure is dramatically different from the other trinuclear (Pt,M,Pt) species of type **XIV**. A noticeable feature is the intramolecular stacking of two $1\text{-}MeT^-$ bases which appears to be related to the lone pair at the central Tl [131].

The Pt coordination planes in these complexes are less distorted than those found in cis dinuclear Pt(II) and Pt(III) species, while the interplanar angles between the Pt and M coordination planes fall in a similar range. In fact, deviations of Pt from the coordination plane range from 0.002 to 0.030 Å and the angles between Pt and M coordination planes from 14.5 to 32.6° (Table 9), whereas in the dinuclear Pt(II),M(II) the corresponding figures vary from 0.01 to 0.19 Å and from 19.3 to

Table 9
Trinuclear h-h *cis*-$[a_2Pt(II)(pym)_2M(pym)_2Pt(II)a_2]^{m+}$ complexes[a]

	Refcode	Pt...M	Pt–N3 Pt–N3 Pt–a Pt–a	M–O4 M–O4	*d*(Pt1)	β	τ	ω	Ref.
$[(NH_3)_2Pt(1\text{-}MeC, N^3, O^2)(1\text{-}MeU^-,N^3,O^4)$ $Cu(II)(1\text{-}MeC,N^3,O^2)(1\text{-}MeU^-,N^3,O^4)Pt(NH_3)_2]^{4+}$	COKRUP	2.681	2.036 2.046 2.080 2.068	1.988[b] 1.932	0.015	77.6	17.8	2.8	[92]
$[(NH_3)_2Pt(1\text{-}MeU^-,N^3, O^4)_2Cu(II)(1\text{-}MeU^-,N^3,$ $O^4)_2Pt(NH_3)_2]^{2+}$	FIDGUU	2.685	2.012 2.018 2.047 2.045	1.929 1.943	0.027	89.2	15.7	3.6	[126]
$[(Me_4en)Pt(1\text{-}MeU^-,N^3, O^4)_2Cu(II)(1\text{-}MeU^-,N^3,$ $O^4)_2Pt(Me_4en)]^{2+}$	KUKHAZ	2.984	2.063 2.035 2.073 2.102	1.927 1.936	0.026	82.1	32.6	21.2	[127]
$[(NH_3)_2Pt(1\text{-}MeT^-,N^3, O^4)_2Mn(II)(1\text{-}MeT^-,N^3,$ $O^4)_2Pt(NH_3)_2]^{2+}$	AMPTMN	2.704	2.017 2.023 2.060 2.020	2.097 2.160	0.018	88.2	20.0	10.5	[128]
$[(NH_3)_2Pt(1\text{-}MeU^-,N^3, O^4)_2Pd(II)(1\text{-}MeU^-,N^3,$ $O^4)_2Pt(NH_3)_2]^{2+}$	VACZOO	2.839	2.042 2.035 2.054 2.068	2.030 2.036	0.002	76.2	21.7	6.7	[129]
	VACZOO	2.836	2.033 2.034 2.060 2.059	2.013 2.017	0.005	81.4	22.6	10.1	

$[(NH_3)_2Pt(1\text{-}MeU^-,N^3,O^4)_2Pd(III)(1\text{-}MeU^-,N^3,O^4)_2Pt(NH_3)_2]^{3+}$	FAWPUO10	2.633	2.034 2.025 2.049 2.044	1.963 1.999	0.004	82.4	14.5	6.5	[130]
$[(NH_3)_2Pt(1\text{-}MeU\ ,N^3,O^4)_2Pd(III)(1\text{-}MeU\ ,N^3,O^4)_2Pt(NH_3)_2]^{3+}$	FAWRAW10	2.641	2.038 2.027 2.050 2.051	1.987 1.998	0.002	87.4	15.4	10.7	[130]
$[(en)Pt(1\text{-}MeT^-,N^3,O^4)_2Pd(III)(1\text{-}MeT^-,N^3,O^4)_2Pt(en)]^{3+}$	VADBEH	2.646	2.031 2.032 2.029 2.015	1.988 1.991	0.004	84.4	16.2	13.6	[129]
$[(NH_3)_2Pt(1\text{-}MeT^-,N^3,O^4)_2Tl(I)(1\text{-}MeT^-,N^3,O^4)_2Pt(NH_3)_2]^{1+}$ [a]	YASXUL	3.085	2.054 2.053 2.042 2.073	2.792 2.921	0.030	79.2	35.3	–	[131]

	Refcode	Pt1...M	M...Pt2	Pt1–N3 Pt1–N3 Pt1–a Pt1–a	M–O4 M–O4 M–O4 M–O4	Pt2–N3 Pt2–N3 Pt2–a Pt2–a	d(Pt1) d(Pt2)	β	τ	ω	Ref.
$[(NH_3)_2Pt(1\text{-}MeT\ ,N^3,O^4)_2Ag(I)(1\text{-}MeT^-,N^3,O^4)_2Pt(NH_3)_2]^{1+}$ [a]	TYMAPT	2.849	2.884	2.026 2.046 2.070 2.067	2.495 2.415 2.348 2.554	2.052 2.041 2.021 2.083	0.021 0.007	77.1 77.2	31.8 28.5	17.0 24.6	[132]

[a] M on a center of symmetry, except for the Pt_2,Tl with Tl located on a two-fold axis and Pt_2,Ag species with Ag on a general position. [b] Cu–O2 distance.

46.5°, the largest values being observed for bulky PMe_3 ligands. This comparison suggests that trinuclear species are less crowded than the dinuclear ones, because the steric interaction between a_2 ligands at Pt and the O donors (at M) in **XIV** is generally smaller than that between facing ligands bonded to two adjacent metal centres in the dinuclear species (Fig. 7, **II** and **III**). Further, when the nature of M allows the four equatorial O donors to be distorted towards a tetrahedral arrangement (as when M is Ag^+ [132]), steric clashes are significantly released.

Therefore, it is not surprising that the previously unprecedented geometry XV (Fig. 11) has recently been reported for a complex with 2-pyridonate (2-pyro), namely *trans*-$[a_2Pt(2\text{-pyro})_2Cu(2\text{-pyro})_2Pta_2]^{2+}$ (a is NH_3 or NH_2Me) [133], with the two 2-pyridonate ligands in the h-h arrangement, and the Cu bound by the exocyclic O atoms. The major strain observed consists of a strong tetrahedral distortion of Cu(II), characterized by O–Cu–O angles slightly above 160°, and likewise a substantial deviation of Pt from an ideal square-planar geometry. The Pt–Cu distances in the two Pt_2Cu complexes, ranging from 2.631 to 2.645 Å, are considerably shorter than those in all structurally characterized compounds Pt_nCu ($n=1$ or 2) derived from *cis*-$[(pym)_2Pta_2]^{2+}$.

Examples with geometry **XIV** both with M is Pd(II) and Pd(III) have been structurally characterized. The compounds of type (Pt, Pd(III), Pt) which contain an unpaired electron per trinuclear unit, are considered models of Pt-pyrimidine blues, with a +2.33 average metal oxidation state [129,130].

As expected, in complexes containing the (Pt, Pd(III), Pt) unit, the Pt–Pd distances are significantly shorter (mean value 2.640 Å) than those found in cations with the (Pt, Pd(II), Pt) core (mean value 2.838 Å). Correspondingly, the Pd(III)–O bonds are shorter than the Pd(II)–O ones by about 0.20 Å. This significant shortening seems to justify formulation of the oxidized compounds as (Pt, Pd(III), Pt).

A linear correlation between Pt–M distances and τ angles, similar to that observed for dinuclear species (Fig. 8), may be derived with a correlation r value of 0.963 for $n=9$ fragments (excluding the Ag and Tl derivatives).

6. Theoretical analysis of the metal–metal interaction

The nature of the metal–metal interaction in homo- and heterobimetallic dimers, described in the previous sections, containing a pair of d^8 metal ions, has been recently investigated [134] with the aid of the extended Hückel method [135] and the fragment molecular orbital theory [136].

The stacked arrangement in 4:4 dimers, containing a pair of d^8 metal ions, such as Pt(II) and/or Pd(II), are stabilized by Rundle-type interactions [137]. Due to *s*, p_z, and z^2 *configuration mixing*, the resulting bond order becomes slightly greater than zero in these formally non-bonded dimers [138]. In other words, the rehybridization of both Pt z^2 orbitals has the effect to stabilize both σ and σ^* MOs, as depicted in Fig. 12, resulting in a net bonding interaction between the two metal ions.

The molecular orbital diagram of the Pt–Pd heterobimetallic compounds of type

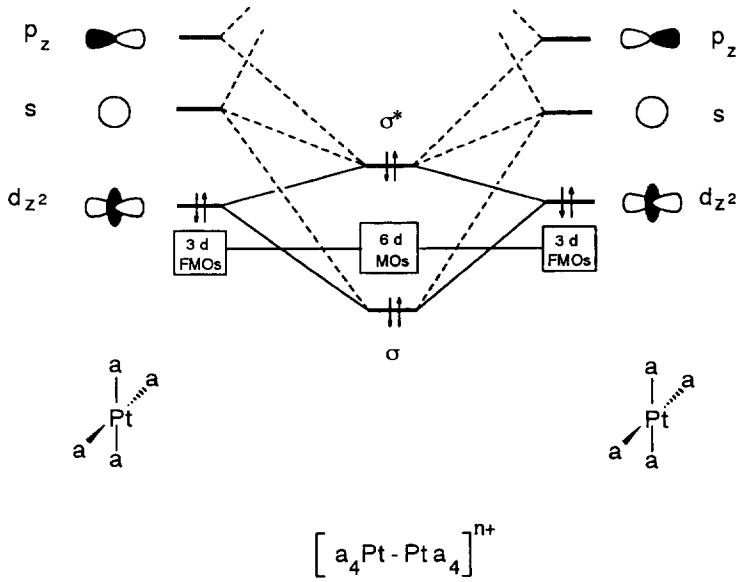

Fig. 12. Pt(II)/d^8-Pt(II)/d^8 molecular orbital diagram for 4:4 type dimers.

4:3 (Fig. 9, **V**), with the so-called *T over square* (TSQ) structural motiv [134], is depicted in Fig. 13. It shows a completely different kind of bonding scheme with respect to the previous one. The strongest interaction, between the square-planar platinum unit (left side), and the T-shaped PdL_3 fragment (right side), involves the Pt z^2 and the Pd x^2–y^2-type FMOs, resulting in a two-electrons/two-orbitals donor acceptor (i.e. dative) bond with a formal bond order of one [134]. Similar conclusions have been reached by other authors on Pt_2 diphosphine bridged dimers [139]. The substitution of the d^8 ion Pd(II) [104,105] with electron richer metal ions, such as d^9-Cu(II) [106] or d^{10}-Hg(II) [107] has the stereoelectronic consequence of weakening the Pt–M interaction in the d^8-d^9 adducts, without destroying the TSQ primary geometry, and of forcing the removal of the ligand coaxial with the metals in d^8-d^{10} adducts. In the d^8-d^9 system a bond order of 0.5 may be suggested; in the d^8-d^{10} the resulting 4:2 type complexes (Fig. 9, **VI**) have a Pt–M bond order only slightly greater then zero [134].

The theoretical calculations allow the trend of the dinuclear Pt–M bond lengths to be rationalized. The values of Pt–Pd distances found in di- and trinuclear species suggest that there is a gradual decrease in bond order from 1 to 0 following the trend (if not otherwise indicated the metal oxidation state is +2):

trans-Pt,Pd	< *cis*-Pt,Pd(III),Pt	< *cis*-Pt,Pd,Pt	< *cis*-Pt,Pd
2.511	2.640	2.838	2.927 Å

The difference between the last two values may be ascribed to differences in steric crowding, although this shortening could also be attributed to electronic factors.

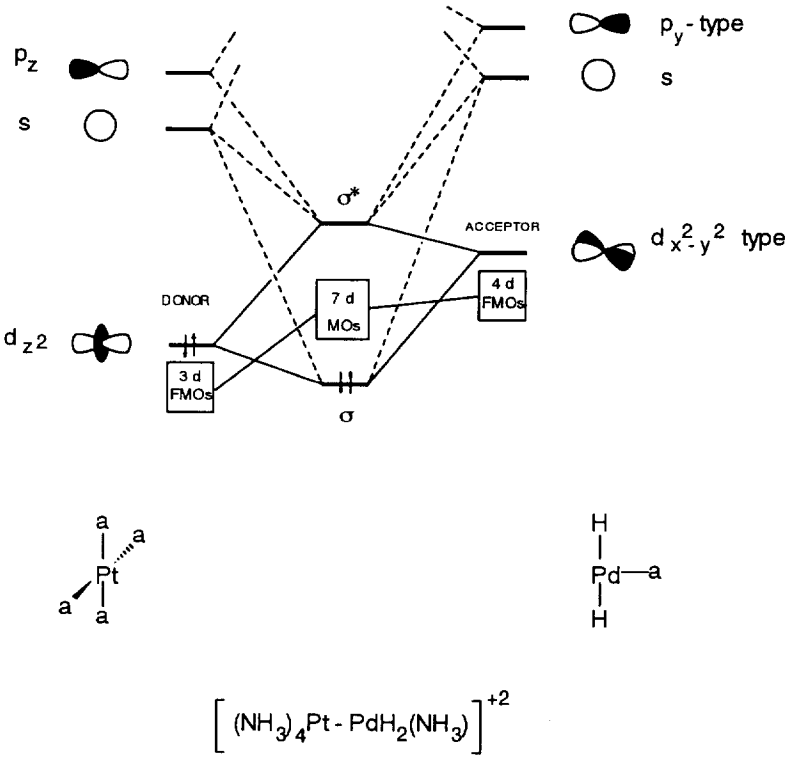

Fig. 13. Pt(II)/d^8-Pd(II)/d^8 molecular orbital diagram for 4:3 type dimers.

More detailed theoretical calculations are required, however, to give a definite answer.

A similar trend, although limited to a few number of derivatives, also seems to hold for the Pt–Cu distances in the analogous copper complexes, with the bond order varying approximately from 0.5 to 0:

trans–Pt,Cu <	*cis*-Pt,Cu,Pt <	*cis*-Pt,Cu
2.500	2.683	2.765 Å

Nevertheless, strong steric interactions caused by bulky ligands at Pt clearly lengthen the Pt–M distances in *cis*-(Pt,M) and *cis*-(Pt,M,Pt) complexes. Thus for example in h-t *cis*-$[(PMe_3)_2Pt(1\text{-}MeC^-,N^3,N^4)_2Pt(PMe_3)_2]^{2+}$ the intermetallic distance is 3.199 Å (Table 5), while in other (Pt,Pt) diamine analogues this distance ranges from 2.861 to 2.981 Å. Similarly, in trinuclear *cis*-$[(Me_4en)\text{-}Pt(1\text{-}MeU^-,N^3,O^4)_2Cu(1\text{-}MeU^-,N^3,O^4)_2Pt(Me_4en)]^{2+}$, the Pt–Cu distance is lengthened to 2.984 Å.

A single Pt–Pt bond can be ascribed to Pt(III) d^7 dimers of type 5:5. Using a simple model, the Pt–Pt bond in the latter complexes may be described as a covalent bond between two d^2sp^3 hybridized d^7 metal ions. A more rigorous approach has

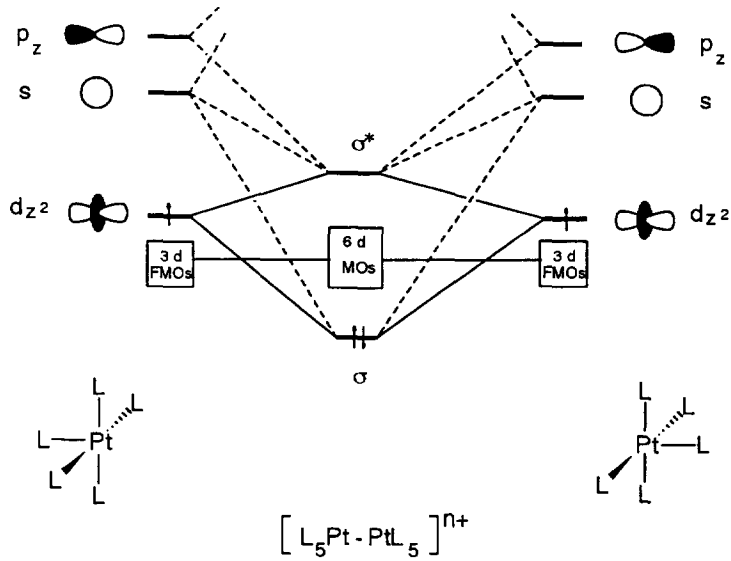

Fig. 14. Pt(III)/d^7-Pt(III)/d^7 molecular orbital diagram for 5:5 type dimers.

been used by Cotton [114], where the single bond is based on a $\sigma^2\pi^4\delta^2\delta^{*2}\pi^{*4}$ configuration, similar to the bonding pattern describing dimers of Rh(II) [137].

The interaction diagram for a L_5Pt–PtL_5, reported in Fig. 14, shows a bonding scheme caused by two electrons/two orbitals (σ and σ^*) interaction between the couple of Pt z^2 frontier orbitals pertained to each PtL_5 fragment. Pt(III) *lantern type* dimers have been described analogously by other authors [125].

7. Polynuclear species

7.1. *Tri- and tetradentate uracilate ligands*

A number of polynuclear Pt, Ag complexes containing uracilate acting as tridentate through O2, N3, and O4, and in one case as tetradentate ligand, through additional binding to O4 (Fig. 15) have been reviewed by Goodgame and Jakubovic in 1987

Fig. 15. 1-Methyluracil anion acting as tridentate and tetradentate ligand.

[140]. These examples demonstrate that the increased basicity of O4 (as a consequence of N3 deprotonation) is sufficient to allow binding of two metals simultaneously. In fact, as already mentioned, metal binding at deprotonated position N3 of 1-MeT$^-$ and 1-MeU$^-$ encourages binding either of an additional metal or of a proton through exocyclic oxygens of these ligands [132,141].

Ag^+ ions seem to be particularly versatile forming polynuclear Pt, Ag complexes, with the metal centers generally approximately collinear and bridged by the nucleobases. Fig. 16 reports a schematic representation of these complexes, while the relevant structural parameters are given in Table 10. The uracilate ligands bridge three adjacent metals in a cis (**XVI**, **XVII** and **XVIII**) or in a trans (**XIX**) arrangement. In the latter additional binding between O4 and Ag ions of adjacent molecules produces a polymeric array of Pt, Ag_2 units [145].

Since then, only one more complex containing the *trans*-$[(MeNH_2)_2Pt(1,5\text{-}Me_2C^-,O^2,N^3,N^4)_2Ag_2]^{2+}$ cation has been structurally characterized [146]. It is the first example of a cytosine metal complex with metal binding simultaneously via N3, N4 (deprotonated) and O2. The h-h arrangement and the solution behaviour of the compound is consistent with the view that the binding of Ag^+ to *trans*-$[(MeNH_2)_2Pt(1,5\text{-}Me_2C)_2]^{2+}$ takes place sequentially, first at N4 sites, then to the O2 sites. The structure of the cation, which is similar to that containing the uracilato base **XIX**, is shown in Fig. 17. Ag–O2 distances are substantially shorter in the case of 1-MeC$^-$ complex (mean value 2.259(8) Å) as compared to 1-MeU$^-$ compounds, where Ag–O2 interactions frequently are very weak (2.4–2.5 Å).

7.2. Purine bases

A unique case of guanine utilizing three metal binding sites is realized in the trinuclear species $\{(9\text{-}EtG^-,N^1,N^3,N^7)[Pt(NH_3)_3]_3\}^{5+}$. In this compound the 9-EtG$^-$ simultaneously binds three $Pt(NH_3)_3$ units through N1, N3, and N7, [147] (**XX**). The platination of the N1 site apparently increases the nucleophilicity of the N3 atom sufficently to become a metal binding site.

In another trinuclear compound of composition *cis*-$[(NH_3)_3Pt\text{-}(9\text{-}MeA,N^1N^7)Pt(NH_3)_2(9\text{-}MeA,N^7,N^1)Pt(NH_3)_3]^{6+}$, two $(NH_3)_3Pt$ residues are bound to N1 and a *cis*-$(NH_3)_2Pt$ entity is bound to N7 of the bases, **XXI** [148]. In the solid state the central Pt is located on a mirror plane with the adenine rings h-h oriented, while in solution an equilibrium between the h-h and h-t rotamers is observed. From ^1H NMR signals a barrier to rotation of $\Delta H \neq 76.5$ kJ mol^{-1} is calculated and this value should be compared with those derived for *cis*-$[(pu)_2Pta_2]$ derivatives [73b].

The Pt–N(pu) bond lengths for these structures are reported in Table 4, together with structures containing bifunctional purine bases.

7.3. Cyclic species

The dinuclear complex *cis*-$[(PMe_3)_2Pt(1\text{-}MeC^-,N^3,N^4)_2Pt(PMe_3)_2]^{2+}$ has been observed to convert slowly, in aqueous or DMSO solution, into a trinuclear species

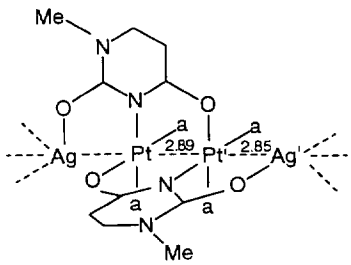

XVI

CIPMUJ

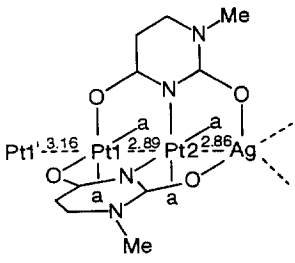

XVII

FOCHEK

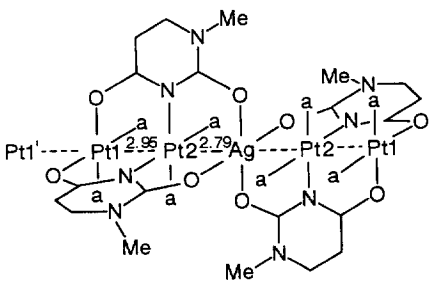

XVIII

BEKKOR

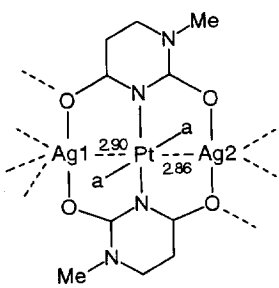

XIX

CICBAR

Fig. 16. Polynuclear Pt, Ag complexes so far structurally characterized with metal–metal distances given.

cis-$[(PMe_3)_2Pt(1\text{-}MeC^-,N^3,N^4]_3^{3+}$ [149]. Three *cis*-$Pt(PMe_3)_2$ units are bridged by the cytosinate anions through N3 and N4 donors to give a trinuclear cation with an approximate C_3 symmetry. The Pt·Pt separation presents a mean value of 5.31 Å.

Table 10
Polinuclear Pt(II),Ag(I) complexes with tri and tetradentate pym ligand (See Fig. 16 for metal–metal distances and atom labels)

	Refcode	Metal coord distances			d(Pt)	β	Ref.
h-h *cis*-[$((NH_3)_4$ $Pt_2(1\text{-}MeU^-,O^4,N^3,O^2)_2)_2Ag]^{5+}$		Pt1	Pt2	Ag			
	BEKKOR	2.085 O4	2.060 N3	2.434 O2	0.038 Pt2	85.2	[142]
		2.088 O4	2.090 N3	2.344 O2	0.111 Pt1		
		2.025	2.067				
		1.989	2.091				
h-h *cis*-[$((NH_3)_4$ $Pt_2(1\text{-}MeU^-,O^4,N^3,O^2)_2)Ag]^{3+}$		Pt1	Pt2	Ag			
	FOCHEK	2.057 O4	2.022 N3	2.357 O2	0.006 Pt2	87.7	[143]
		2.028 O4	2.068 N3	2.468 O2	0.080 Pt1		
		2.014	2.029	2.329[a]			
		2.002	2.057	2.376[a]			
h-t *cis*-[$(NH_3)_4Pt_2(1\text{-}MeU^-,O^4,N^3,O^2)_2Ag_2]^{4+}$		Pt	Pt′	Ag′			
	CIPMUJ	2.025 N3	2.037 O4	2.386 O2	0.039	81.3	[144]
		2.037 O4	2.025 N3	2.422[a]			
		2.045	2.045				
		2.015	2.015				
h-t *trans*-[$(NH_3)_2Pt(1\text{-}MeU^-,O^4,N^3,O^2)_2Ag_2]^{2+}$		Ag1	Pt	Ag2			
	CICBAR	2.326 O2	2.084 N3	2.314 O4	0.033	6.1	[145]
		2.239 O4	1.984 N3	2.447 O2			
		2.419[b]	2.132	2.411[a]			
			2.028	2.368[c]			
h-h *trans*-[$(NH_2Me)_2Pt(1,5\text{-}Me_2C^-,O^2,N^3,N^4)_2Ag_2]^{2+}$		Ag1	Pt	Ag2			
	*	2.259 O2	2.039 N3	2.172 N4	0.003	1.7	[146]
		2.259 O2	2.045 N3	2.149 N4			
			2.052				
			2.036				

[a] Ag–ONO_2 contact. [b] Ag–OH_2 distance. [c] Ag–O4′ of an adjacent cation.

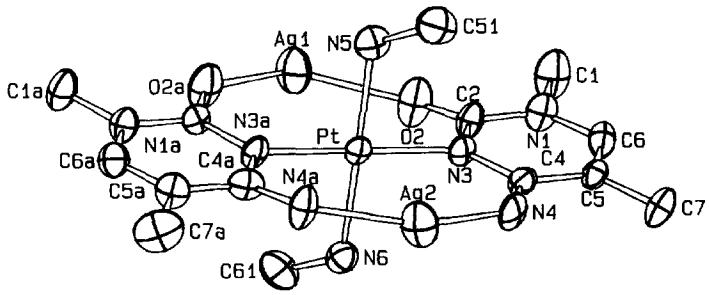

Fig. 17. ORTEP drawing of trinuclear cation *trans*-$[(MeNH_2)_2Pt(1,5\text{-}Me_2C^-,O^2,N^3,N^4)_2Ag_2]^{2+}$.

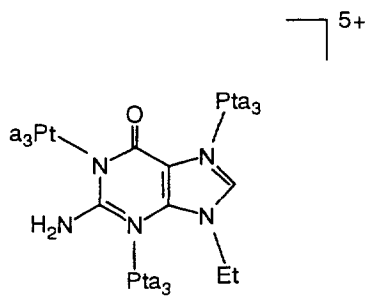

XX

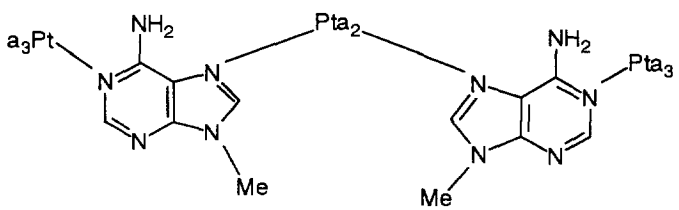

XXI

The trimerization reaction possibly is a consequence of lower intramolecular repulsion of the *cis*-$Pt(PMe_3)_2$ units when compared with a dinuclear arrangement.

The same authors recently investigated the interaction of the model 9-MeGH with *cis*-$[(PMe_3)_2Pt(NO_3)_2]$ at neutral pH, obtaining a hexameric cyclic cation *cis*-$[(PMe_3)_2Pt(9\text{-}MeG^-,N^1,N^7)]_6{}^{6+}$ [65]. It represents a rare example of a hexanuclear platinum nucleobase complex [150]. The hexamer exhibits the purine rings alternatively arranged above and below the mean plane passing through the metal atoms,

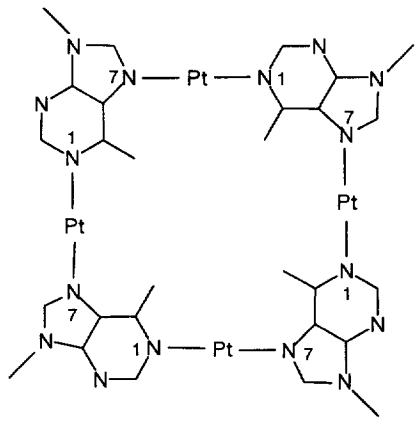

Fig. 18. Hypothesized arrangements for cyclic purine nucleobase quartets.

forming an angle of 50° with the latter. The distance between two adjacent Pt atoms is 6.5 Å.

A tetranuclear species $[(en)Pt(UH^-,N^1,N^3)]_4^{4+}$, that can be considered a metal analogue of the classical calix[4]arene, formed spontaneously from the mononuclear

precursor $[(en)Pt(UH^-,N^1)(H_2O)]^+$, has been reported [151]. The four (en)Pt moieties occupy the corners of a square (Pt·Pt distance 5.86 Å), with the uracil ligands bridging each side alternatively above and below the Pt_4 plane in a 1,3 alternate conformation. The uracil monoanions adopt rare tautomeric forms in that both N1 and N3 sites are platinated and the acidic proton is bound either to O2 or O4. In solution the complex is conformationally flexible and different cations (such as Ag^+) affect the equilibria among the conformers [37,151].

From examples reported in this and previous sections, it is evident that the sequential application of different metal species with nucleic acids can lead to larger aggregates. Formation of cyclic nucleobase quartets (Fig. 18) are proposed on the basis of the crystal structure of *trans*-$[(NH_2Me)_2ClPt(9\text{-}MeA,N^1,N^7)]_2(NH_3)_2Pt^{2+}$ [78] which can be considered a precursor for future extension work. The two vectors ClPtN(nb) in the cited structure are about at right angles to each other, facilitating (in principle) a coplanar arrangement of four purine bases connected by four metal ions with linear coordination (Fig. 18). In contrast, for steric reasons, similar cyclic species with coplanar bases cannot be obtained starting from *cis*-$[(nb)_2Pta_2]$ complexes because large dihedral angles between the nucleobases are to be expected. In fact, in the cited $[(en)Pt(UH^-,N^1,N^3)]_4{}^{4+}$ the four bases are approximately at right angles [37,151].

8. Miscellaneous

Although there are many structures of complexes containing the 9-substituted guanine bound to Pt through N7 or N1 or both, only in the dinuclear decanegative anion $[(G^{2-})Pt(\mu\text{-}PO_4)_4Pt(G^{2-})]^{10-}$, the base is coordinated to Pt(III) through N9, the protons N9–H and N1–H being missing. The Pt–N9(guanine) axial distances of 2.141(2) Å are long due to the high trans influence of the Pt–Pt bond. The intermetallic distance is 2.5342(4) Å [152].

9. Statistical analysis

9.1. Data retrieval

The CSD [22], version 5.08 of October 1994, was searched for Pt–nucleobase compounds, using the QUEST program. Subsequently the following subsets were retrieved by using the RETFIL program [153]:

(a) mononuclear Pt(II) complexes with monofunctional nucleobase:
cytosine and thymine/uracil bound through N3;
all pyrimidine bases bound through N3;
guanine and adenine bound through N7;
all purine bases bound through N7 and through N1;

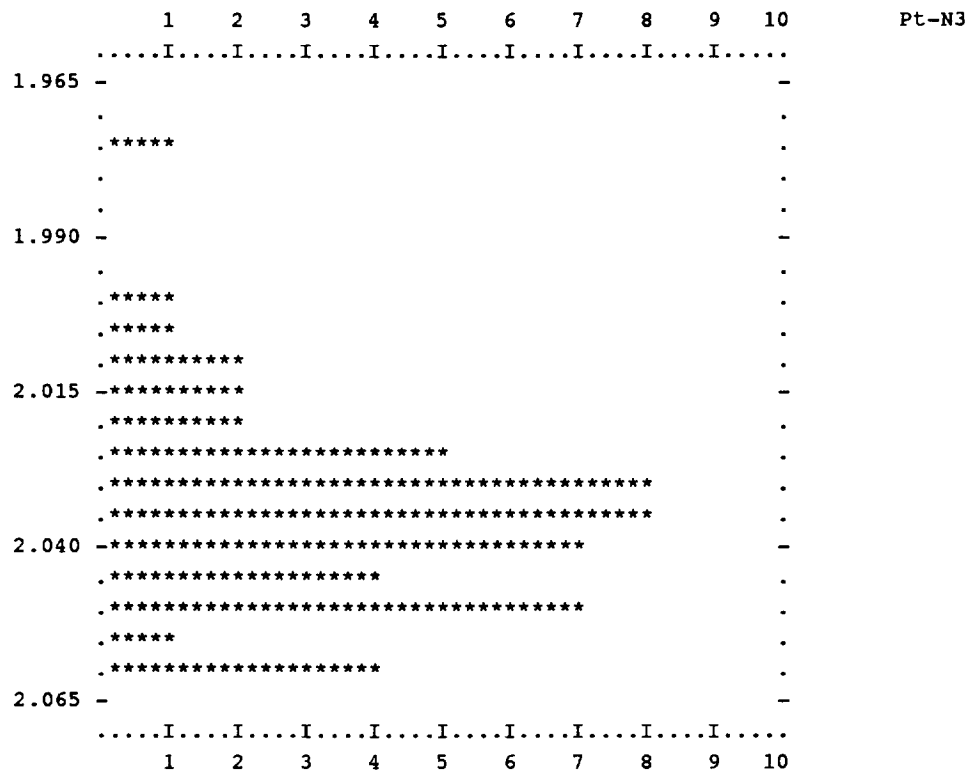

Fig. 19. Histogram of Pt–N3 distances in complexes containing monofunctional pyrimidines.

(b) dinuclear complexes with two cis bridging nucleobases:
Pt(II)–Pt(II) of type 4:4;
Pt(II)–M of type 4:4 (M is Pt,Pd) and 4:5 (M is Cu or Zn);
Pt(III)–Pt(III) of type 4:5 and 5:5;
(c) trinuclear complexes of type Pt–M–Pt (M is Cu(II), Mn(II), Pd(II), Pd(III)).

9.2. Geometrical analysis

The GEOSTAT program [153] was used for an univariate analysis of geometrical parameters for each subset. No particular restrictions were placed, since only a few crystal structures have a discrepancy R factor larger then 0.07. Histograms and scatterplots were obtained from CSD software. The relevant calculated parameters for the different molecular fragments were

(a) Pt–N3 (or Pt–N7) bond length;
displacement of Pt from coordination mean plane, d (absolute value);
displacement of Pt from mean nucleobase plane, d_B (absolute value);
dihedral angle between platinum coordination mean plane and backbone

nucleobase plane (α). If this angle was larger than 90°, its complementary value was taken.

angles around N3 (or N7) donor atom;

(b, c) metal–metal distances;

dihedral angle between adjacent metal coordination planes (τ);

average torsion angle about the Pt–Pt (or Pt–M) vector (ω)

9.3. Results

The mean value (with the standard error of the mean in parentheses), the range, the sample standard deviation (SD), and the number of observations for each parameter are reported in Tables 11 and 12.

The coordination distance Pt–N3 in complexes containing cytosine nucleobases are close to the corresponding value in thymine and uracil derivatives, as well as for the Pt–N7 distances in complexes of adenine similar to those of guanine, despite of the nature and number of substituents on the ring. The calculated mean value

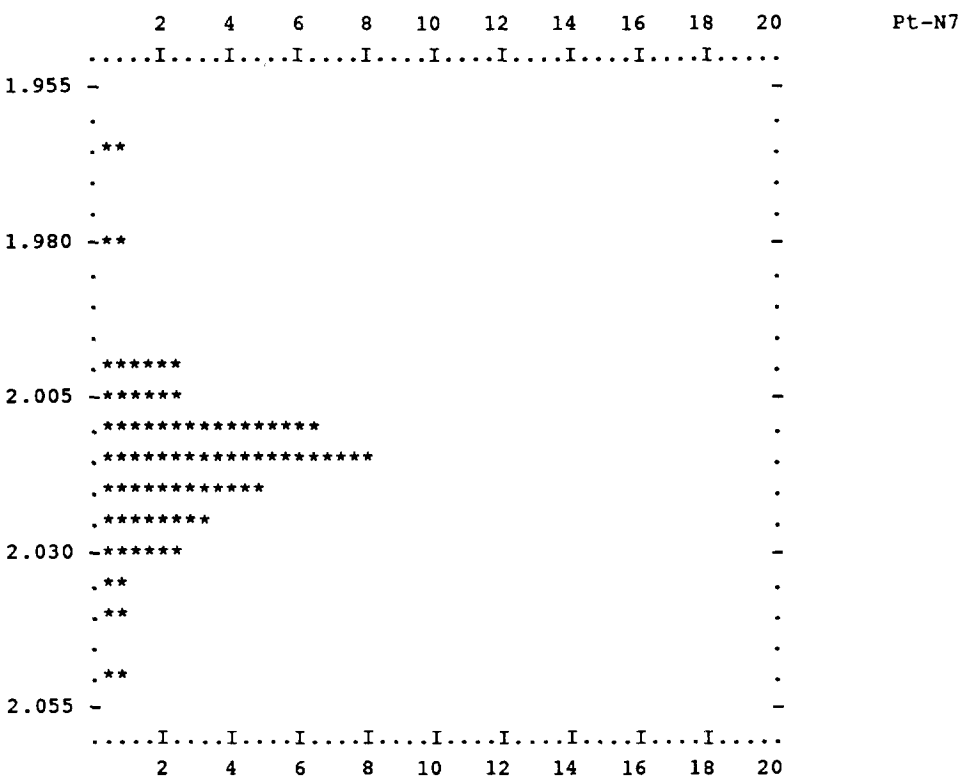

Fig. 20. Histogram of Pt–N7 distances in complexes containing mono- and difunctional purines.

Table 11
Mean Pt–N(nb) bond lengths (Å), angles (°) around the N-donor, displacements (Å) of Pt from the coordination and from the nucleobase plane

	Mean value	Min	Max	S.D.	*n* obs.
cystosine,N^3					
Pt-N3	2.035(2)	2.004	2.059	0.014	37
Pt-N3-C2	116.7(2)	113.9	118.9	1.3	
Pt-N3-C4	122.5(3)	118.5	125.8	1.6	
C2-N3-C4	120.7(2)	118.4	123.4	1.1	
α	80(1)	62.7	89.4	6.2	
d	0.015(2)	0.000	0.040	0.012	
d_B	0.14(2)	0.005	0.322	0.093	
thymine/uracil,N^3					
Pt-N3	2.031(6)	1.973	2.059	0.022	16
Pt-N3-C2	118.2(6)	114.2	122.8	2.3	
Pt-N3-C4	119.6(6)	114.7	123.4	2.5	
C2-N3-C4	122.0(3)	118.8	123.4	1.3	
α	76(3)	60.3	89.7	10.0	
d	0.021(5)	0.000	0.049	0.018	
d_B	0.16(3)	0.009	0.456	0.126	
pyrimidine,N^3					
Pt-N3	2.034(2)	1.973	2.059	0.017	53
thymine/uracil,N^1					
Pt-N1	2.032(5)	2.019	2.040	0.009	4
guanine,N^7					
Pt-N7	2.017(3)	1.963	2.050	0.015	29
Pt-N7-C5	127.9(6)	122.2	135.8	3.3	
Pt-N7-C8	125.6(6)	118.7	131.4	3.0	
C5-N7-C8	106.0(3)	101.8	109.5	1.4	
α	70(3)	41.4	88.2	14.0	
d	0.021(3)	0.000	0.056	0.018	
d_B	0.19(3)	0.000	0.491	0.158	
adenine,N^7					
Pt-N7	2.010(4)	1.978	2.040	0.014	13
Pt-N7-C5	127.7(5)	124.8	130.3	1.8	
Pt-N7-C8	126.2(7)	120.6	129.7	2.6	
C5-N7-C8	106.0(6)	103.3	113.1	2.3	
α	79(3)	62.4	89.6	9.3	
d	0.017(3)	0.005	0.034	0.009	
d_B	0.12(2)	0.005	0.236	0.077	
purine,N^7					
Pt-N7	2.015(2)	1.963	2.050	0.015	42
purine,N^1					
Pt-N1	2.041(5)	2.004	2.061	0.016	10
Pt-N1-C2	119(1)	113.7	124.2	3.5	
Pt-N1-C6	120(1)	115.2	125.0	3.5	
C2-N1-C6	121.0(5)	116.4	123.7	1.8	
α	75(4)	58.6	89.9	11.9	
d	0.39(6)	0.000	0.062	0.020	
d_B	0.22(5)	0.024	0.584	0.171	

Table 12
Mean values of metal-metal distance (Å), tilt angle τ (°) between adjacent metal coordination planes and average torsion (or twist) angle ω (°) about the Pt–M vector in di- and trinuclear complexes[a]

	Mean value	Min	Max	S.D.	*n* obs.
Pt–Pt					
Pt–Pt	2.96(3)	2.861	3.199	0.086	11
τ	34(2)	22.5	46.5	5.8	
ω	13(2)	1.8	24.4	8.1	
Pt–M (M = Pt, Pd, Cu, Zn)					
Pt–M	2.93(3)	2.760	3.199	0.103	14
τ	32(2)	19.3	46.5	6.6	
ω	13(2)	1.8	24.4	7.3	
Pt–M–Pt (M = Cu, Mn, Pd, Pd(III))					
Pt–M	2.74(3)	2.633	2.984	0.117	9
τ	20(1)	14.5	32.6	5.5	
ω	10(1)	2.8	21.2	5.5	
Pt(III)–Pt(III)					
Pt–Pt	2.60(2)	2.543	2.699	0.056	9
τ	20.7(7)	16.0	23.2	2.2	
ω	22(3)	3.1	29.8	10.1	

[a] Oxidation state of metals is +2, unless otherwise indicated.

[2.034(2) Å] for the Pt–N3(pym) is significantly longer than that found in Pt–N7(pu) [2.015(2) Å], but similar to the mean of Pt–N1(pym), the latter derived from four observations. A mean value of 2.041(5) Å has been calculated for the Pt–N1(pu) bond lengths. The difference can be ascribed to the different size of the ring containing the N donor atom. A visual display of the Pt–N3(pym) and Pt–N7(pu) distances is reported in histograms of Fig. 19 and Fig. 20.

In thymine and uracil complexes the Pt–N3–C bond angles are equal (within the standard error of the mean), while in cytosine the angle on the side of amino group appears larger with respect to that (C2–N3–Pt) on the side of C=O group. In purine complexes the coordination Pt–N–C angles present essencially the same value, both for N7 and N1.

The displacement of Pt from the nucleobase mean plane, d_B, falls in a range of approx. 0.5 Å, in complexes both with pym and pu bases. The value might be influenced in some cases by the crystal packing. We do not want to speculate on this parameter, although the d_B values have been used in molecular mechanics calculations for the development of a suitable force field to model DNA–*cis*-Pta_2 adducts [14]. Histograms of d_B for pyrimidine N3 and purine N7 coordinated are reported in Figs. 21 and 22, respectively. In contrast, the coordination out-of-plane of Pt, which is reported for mononuclear Pt(II) complexes in Tables 1 and 2, falls in a narrower range (0–0.05 Å).

The results of the geometrical parameters for di- and trinuclear complexes

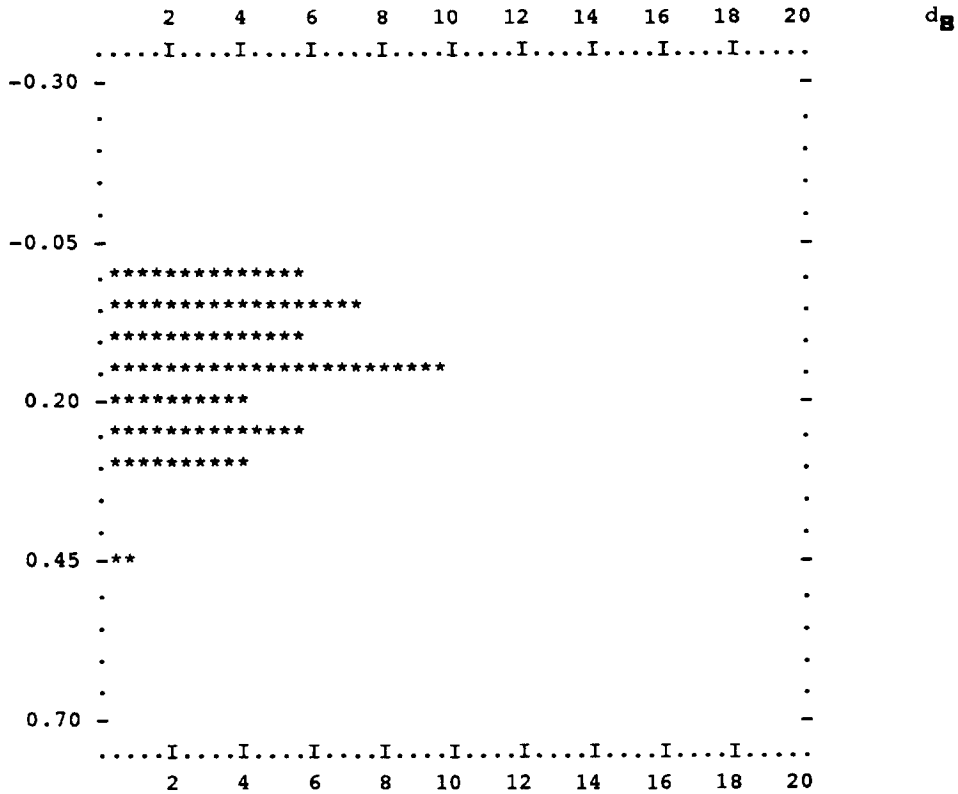

Fig. 21. Histogram for displacement of Pt from pyrimidine ring, d_B.

(Table 12) have been reported and discussed in the sections devoted to these species.

10. Conclusions

The aim of this review is not only to present a detailed factual survey of Pt complexes with nucleobases in solid state, but also to examine some fundamental implications of structure with their chemical behaviour. Structural data such as bond lengths, angular distortions in the metal coordination sphere or at the nucleobase binding site, metal out-of-plane, torsional angles etc. can be derived for these compounds with relatively high accuracy. Apart from unambiguously confirming Pt binding sites at nucleobases (an aspect of particular importance if previously controversial), X-ray crystallography provides detailed structural information which should be useful, among others, in theoretical studies (molecular mechanics, molecular dynamics) of Pt–DNA interactions, particularly concerning the antitumor cisplatin-like agents.

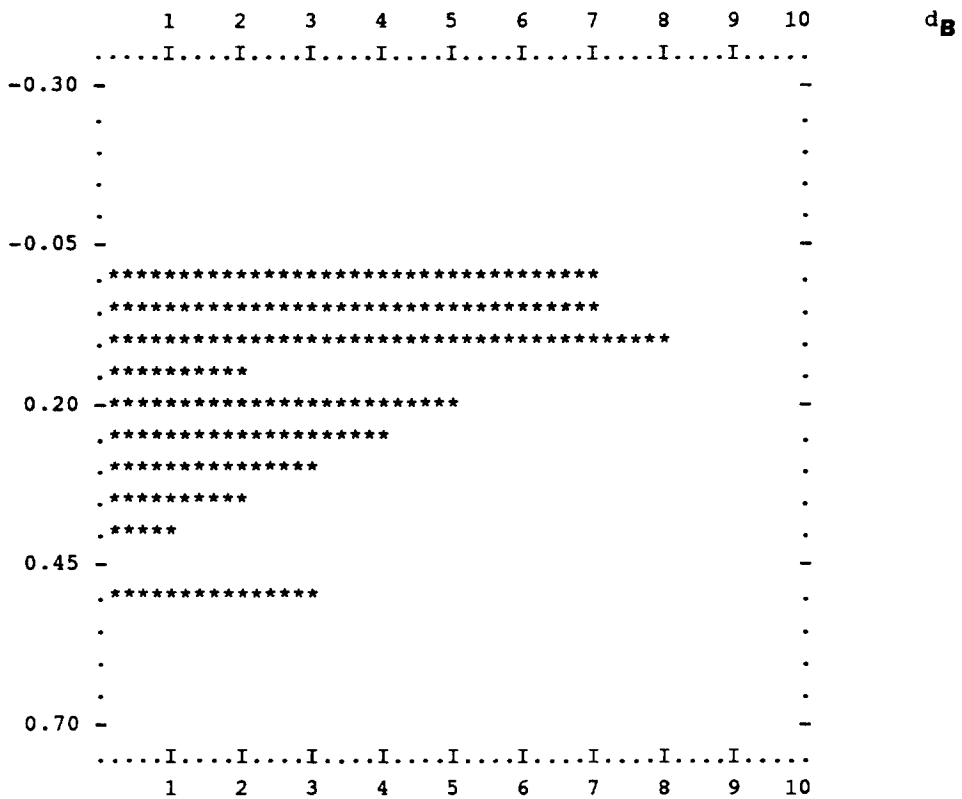

Fig. 22. Histogram for displacement of Pt from purine ring, d_B.

A special focus of the review is devoted to polynuclear complexes containing either Pt alone or in combination with one or more heterometal ions. Multiple metal ion binding to nucleobases has began to emerge as an outstanding feature especially of pyrimidine nucleobase coordination chemistry. The metal–metal interaction is rather variable in these complexes and it can be often highlighted and interpreted applying semiempirical MO methods.

Appendix 1.

List of abbreviations

A	adenine, unspecified
C	cytosine, unspecified or neutral form
G	guanine, unspecified
T	thymine, unspecified
nb	generic nucleobase
pym	pyrimidine
pu	purine
h-h	head–head arrangement
h-t	head–tail arrangement
L, X, Y	generic ligands
a	NH_3 amine
1-MeC	1-methylcytosine
1-MeC$^-$	1-methylcytosinate, N4 deprotonated
1,5-Me_2C^-	1,5-dimethylcytosinate, N4 deprotonated
1-MeTH	1-methylthymine
4H, 1-MeTH	2-oxo-4-hydroxo form of neutral 1-methylthymine
1-MeT$^-$	1-methylthyminate, N3 deprotonated
1-TH$^-$	thyminate
1-MeUH	1-methyluracil
4H, 1-MeUH	2-oxo-4-hydroxo form of neutral 1-methyluracil
1-MeU$^-$	1-methyluracilate, N3 deprotonated
UH$^-$	uracilate
3-MeA	3-methyladenine
9-MeA	9-methyladenine
9-MeAH$^+$	9-methyladeninium
1,9-Me_2AH^+	1,9-dimethyladeninium
6,9-Me_2AH^+	6,9-dimethyladeninium
9-EtGH	9-ethylguanine
9-EtG$^-$	9-ethylguanine anion
9-$MeGH_2^+$	9-methylguaninium
7,9-Me_2G	7,9-dimethylguanine
N^1, N^3, O^4, etc.	sites of coordination
Me	methyl
Et	ethyl
bmik	bis(*N*-methylimidazol-2-yl)ketone
bipy	2,2′-bipyridyl
dien	diethylenetriamine
Gly	glycinate anion
Cp	cyclopentadienyl
en	ethylenediamine
Me_4en	tetramethylethylenediamine

NH_2Me	methylamine
$pymS^-$	2-thiopyrimidinato
TU^-	2-thiouracilato
2-pyro	2-pyridonato
pyz	pyrazine
DMSO	*N*,*N*-dimethylsulphoxide
DMF	*N*,*N*-dimethylformamide

References

[1] B. Rosenberg, L. VanCamp, J.E. Trosko and V.H. Mansour, Nature, 222 (1969) 385.
[2] B. Rosenberg, Naturwissenschaften, 60 (1973) 399.
[3] Abstract Book, 7th Int. Symp. Platinum and Other Metal Coord. Comp. Cancer Chemother., Amsterdam, 1995.
[4] D.P. Bancroft, C.A. Lepre and S.J. Lippard, J. Am. Chem. Soc., 112 (1990) 6860.
[5] L.S. Hollis, A.R. Amundsen and E.W. Stern, J. Med. Chem., 32 (1989) 128.
[6] A.M.J. Fichtinger-Schepman, J.L. van der Veer, J.H.J. den Hartog, P.H.M. Lohmann and J. Reedijk, Biochemistry, 24 (1985) 707.
[7] A. Eastman, Biochemistry, 24 (1985) 5027.
[8] (a) S.E. Sherman, D. Gibson, A.H.-J. Wang and S.J. Lippard, Science, 230 (1985) 412; (b) S.E. Sherman, D. Gibson, A.H.-J. Wang and S.J. Lippard, J. Am. Chem. Soc., 110 (1988) 7368.
[9] G. Admiraal, J.L. van der Veer, R.A.G. de Graaff, J.H.J. den Hartog and J. Reedijk, J. Am. Chem. Soc., 109 (1987) 592.
[10] F. Herman, J. Kozelka, V. Stoven, E. Guittet, J.-P. Girault, T. Huynh-Dinh, J. Igolen, J.-Y. Lallemand and J.-C. Chottard, Eur. J. Biochem., 194 (1990) 119.
[11] S.F. Bellon, J.H. Coleman and S.J. Lippard, Biochemistry, 30 (1991) 8026.
[12] S.L. Bruhn, J.H. Toney and S.J. Lippard, Progr. Inorg. Chem., 38 (1990) 477.
[13] D. Kiser, F.P. Intini, Y. Xu, G. Natile and L.G. Marzilli, Inorg. Chem., 33 (1994) 4149.
[14] S. Yao, J.P. Plastaras and L.G. Marzilli, Inorg. Chem., 33 (1994) 6061.
[15] B. Lippert, G. Raudaschl-Sieber, C.J.L. Lock and P. Pilon, Inorg. Chim. Acta, 93 (1984) 43.
[16] H. Schöllhorn, G. Raudaschl-Sieber, G. Müller, U. Thewalt and B. Lippert, J. Am. Chem. Soc., 107 (1985) 5932.
[17] B. Lippert, Prog. Inorg. Chem., 37 (1989) 1.
[18] J.R. Lusty (Ed.) Handbook of Nucleobase Complexes, Vol. I, CRC Press, Boca Raton, FL, 1990.
[19] J.R. Lusty, P. Wearden and V. Moreno (Eds.), Handbook of Nucleobase Complexes, Vol. II, CRC Press, Boca Raton, FL, 1992.
[20] R. Faggiani, C.J.L. Lock and B. Lippert, Inorg. Chim. Acta, 106 (1985) 75.
[21] H.-J. Korte and R. Bau, Inorg. Chim. Acta, 79 (1983) 251.
[22] F.H. Allen, J.E. Davies, J.J. Galloy, O. Johnson, O. Kennard, C.F. Macrae, E.M. Mitchell, G.F. Mitchell, J.M. Smith and D.G. Watson, J. Chem. Info. Comp. Sci., 31 (1991) 187.
[23] J.F. Britten, B. Lippert, C.J.L. Lock and P. Pilon, Inorg. Chem., 21 (1982) 1936.
[24] B. Lippert, C.J.L. Lock and R.A. Speranzini, Inorg. Chem., 20 (1981) 335.
[25] H. Schollhorn, U. Thewalt, G. Raudaschl-Sieber and B. Lippert, Inorg. Chim. Acta, 124 (1986) 207.
[26] C.J.L. Lock, R.A. Speranzini and J. Powell, Can. J. Chem., 54 (1976) 53.
[27] H. Preut, G. Frommer and B. Lippert, Acta Crystallogr. Sect. C, 46 (1990) 1326.
[28] B. Lippert, C.J.L. Lock and R.A. Speranzini, Inorg. Chem., 20 (1981) 808.
[29] F.J. Pesch, H. Preut and B. Lippert, Inorg. Chim. Acta, 169 (1990) 195.
[30] A. Iakovidis, N. Hadjiliadis, J.F. Britten, I.S. Butler, F. Schwarz and B. Lippert, Inorg. Chim. Acta, 184 (1991) 209.

[31] F. Schwarz, H. Schollhorn, U. Thewalt and B. Lippert, J. Chem. Soc. Chem. Commun., (1990) 1282.
[32] S. Jaworski, H. Schollhorn, P. Eisenmann, U. Thewalt and B. Lippert, Inorg. Chim. Acta, 153 (1988) 31.
[33] L.S. Hollis, A.R. Amundsen and E.W. Stern, J. Med. Chem., 32 (1989) 128.
[34] H. Schollhorn, U. Thewalt and B. Lippert, Inorg. Chim. Acta, 106 (1985) 177.
[35] G. Bandoli, G. Trovo, A. Dolmella and B. Longato, Inorg. Chem., 31 (1992) 45.
[36] R. Faggiani, B. Lippert and C.J.L. Lock, Inorg. Chem., 19 (1980) 295.
[37] H. Rauter, E.C. Hillgeris, A. Erxleben and B. Lippert, J. Am. Chem. Soc., 116 (1994) 616.
[38] F. Schwarz, B. Lippert, H. Schollhorn and U. Thewalt, Inorg. Chim. Acta, 176 (1990) 113.
[39] B. de Castro, C.C. Chiang, K. Wilkowski, L.G. Marzilli and T.J. Kistenmacher, Inorg. Chem., 20 (1981) 1835.
[40] A. Terzis, Inorg. Chem., 15 (1976) 793.
[41] R. Beyerle-Pfnur, S. Jaworski, B. Lippert, H. Schollhorn and U. Thewalt, Inorg. Chim. Acta, 107 (1985) 217.
[42] B. Lippert, H. Schollhorn and U. Thewalt, Inorg. Chim. Acta, 198 (1992) 723.
[43] A. Terzis and D. Mentzafos, Inorg. Chem., 22 (1983) 1140.
[44] J.D. Orbell, C. Solorzano, L.G. Marzilli and T.J. Kistenmacher, Inorg. Chem., 21 (1982) 3806.
[45] L. Cavallo, R. Cini, J. Kobe, L.G. Marzilli and G. Natile, J. Chem. Soc. Dalton Trans., (1991) 1867.
[46] W.S. Sheldrick and G. Heeb, Inorg. Chim. Acta, 190 (1991) 241.
[47] UH^- and TH^- indicate anions deprotonated either at N1 or at N3, but the ambiguity is removed by the indication of the coordination site.
[48] J.D. Orbell, L.G. Marzilli and T.J. Kistenmacher, J. Am. Chem. Soc., 103 (1981) 5126.
[49] R. Faggiani, B. Lippert and C.J.L. Lock, Inorg. Chem., 21 (1982) 3210.
[50] H. Preut, G. Frommer and B. Lippert, Acta Crystallogr. Sect. C, 47 (1991) 852.
[51] M. Grehl and B. Krebs, Inorg. Chem., 33 (1994) 3877.
[52] O. Renn, B. Lippert and A. Albinati, Inorg. Chim. Acta, 190 (1991) 285.
[53] O. Renn, B. Lippert, H. Schollhorn and U. Thewalt, Inorg. Chim. Acta, 167 (1990) 123.
[54] D. Neugebauer and B. Lippert, J. Am. Chem. Soc., 104 (1982) 6596.
[55] H. Schollhorn, U. Thewalt and B. Lippert, J. Am. Chem. Soc., 111 (1989) 7213.
[56] R. Faggiani, B. Lippert, C.J.L. Lock and R. Pfab, Inorg. Chem., 20 (1981) 2381.
[57] B. Lippert, R. Pfab and D. Neugebauer, Inorg. Chim. Acta, 37 (1979) L495.
[58] B.E. Brown and C.J.L. Lock, Acta Crystallogr. Sect. C, 44 (1988) 611.
[59] G. Frommer, I. Mutikainen, F.J. Pesch, E.C. Hillgeris, H. Preut and B. Lippert, Inorg. Chem., 31 (1992) 2429.
[60] J.D. Orbell, C. Solorzano, L.G. Marzilli and T.J. Kistenmacher, Inorg. Chem., 21 (1982) 2630.
[61] A. Iakovidis, N. Hadjiliadis, F. Dahan, J.-P. Laussac and B. Lippert, Inorg. Chim. Acta, 175 (1990) 57.
[62] H. Schollhorn, G. Raudaschl-Sieber, G. Muller, U. Thewalt and B. Lippert, J. Am. Chem. Soc., 107 (1985) 5932.
[63] L. Sindellari, H. Schollhorn, U. Thewalt, G. Raudaschl-Sieber and B. Lippert, Inorg. Chim. Acta, 168 (1990) 27.
[64] J.D. Orbell, M. R. Taylor, S.L. Birch, S.E. Lawton, L.M. Vilkins and L.J. Keefe, Inorg. Chim. Acta, 152 (1988) 125.
[65] B. Longato, G. Bandoli, G. Trovò, E. Marasciulo and G. Valle, Inorg. Chem., 34 (1995) 1745.
[66] F.J. Pesch, M. Wienken, H. Preut, A. Tenten and B. Lippert, Inorg. Chim. Acta, 197 (1992) 243.
[67] R. Beyerle-Pfnur, B. Brown, R. Faggiani, B. Lippert and C.J.L. Lock, Inorg. Chem., 24 (1985) 4001.
[68] R. Faggiani, B. Lippert, C.J.L. Lock and R.A. Speranzini, Inorg. Chem., 21 (1982) 3216.
[69] I. Dieter-Wurm, M. Sabat and B. Lippert, J. Am. Chem. Soc., 114 (1992) 357.
[70] O. Krizanovic, M. Sabat, R. Beyerle-Pfnur and B. Lippert, J. Am. Chem. Soc., 115 (1993) 5538.
[71] For purine bases N1 and N9 coordinated the calculated torsional angles are C2–N1–Pt–N1 and C8–N9–Pt–N9, respectively.

[72] R.E. Cramer and P.L. Dahlstrom, J. Am. Chem. Soc., 101 (1979) 3679.
[73] (a) M.D.Reily and L.G. Marzilli, J. Am. Chem. Soc., 108 (1986) 6785; (b) D. Li and R.N. Bose, J. Chem. Soc. Dalton Trans., (1994) 3717
[74] T.J. Kistenmacher, J.D. Orbell and L.G. Marzilli, Conformational properties of purine and pyrimidine complexes of cisplatinum in S.J. Lippard (Ed.), Platinum, Gold, and Other Metal Chemotherapeutic Agents, ACS Symp. Ser. 209, 1983, p. 191.
[75] D. Holthenrich, I. Sóvágó, A. Erxleben, G. Fusch, E.C. Fusch and B. Lippert, Z. Naturforsch. Teil B, 50 (1995) 1767.
[76] J. Reedijk, J.H.J den Hartog, A.M.J. Fichtinger-Schepman and A.T.M. Marcelisin, in M.P. Hacker, E.B. Douple, I.H. Krakoff (Eds.), Platinum Coordination Complexes in Cancer Chemotherapy, Martinus Nijhoff, Boston, 1984, p. 39.
[77] T.W. Hambley, Inorg. Chem., 27 (1988) 1073.
[78] A. Schreiber, E. Hillgeris and B. Lippert, Z. Naturforsch. Teil B, 48 (1993) 1603.
[79] F.D. Rochon, P.C. Kong and R. Melanson, Can. J. Chem., 59 (1981) 195.
[80] D. Holthenrich, E. Zangrando, F. Pichierri, L. Randaccio, B. Lippert, Inorg. Chim. Acta, 248 (1996) 175.
[81] H. Schollhorn, R. Beyerle-Pfnur, U. Thewalt and B. Lippert, J. Am. Chem. Soc., 108 (1986) 3680.
[82] G. Muller, J. Riede, R. Beyerle-Pfnur and B. Lippert, J. Am. Chem. Soc., 106 (1984) 7999.
[83] G. Frommer, H. Preut and B. Lippert, Inorg. Chim. Acta, 193 (1992) 111.
[84] I. Dieter, B. Lippert, H. Schollhorn and U. Thewalt, Z. Naturforsch. Teil B, 45 (1990) 731.
[85] B. Lippert, H. Schollhorn and U. Thewalt, J. Am. Chem. Soc., 108 (1986) 6616.
[86] The U derivatives were produced by the oxidation agents used in the reactions.
[87] G. Frommer, H. Schollhorn, U. Thewalt and B. Lippert, Inorg. Chem., 29 (1990)1417.
[88] C.J.L. Lock, R.A. Speranzini, G.Turner and J. Powell, J. Am. Chem. Soc., 98 (1976) 7865.
[89] W. Micklitz, O. Renn, H. Schollhorn, U. Thewalt and B. Lippert, Inorg. Chem., 29 (1990) 1836.
[90] A.L. Balch and V.J. Catalano, Inorg. Chem., 31 (1992) 3934.
[91] H. Schollhorn, U. Thewalt and B. Lippert, Inorg. Chim. Acta, 135 (1987) 155.
[92] B. Lippert, U. Thewalt, H. Schollhorn, D.M.L. Goodgame and R.W. Rollins, Inorg. Chem., 23 (1984) 2807.
[93] a) B. Lippert, D. Neugebauer and U. Schubert, Inorg. Chim. Acta, 46 (1980) L11; (b) H. Schollhorn, U. Thewalt and B. Lippert, Inorg. Chim. Acta, 93 (1984) 19.
[94] B. Lippert, D. Neugebauer, G. Raudaschl, Inorg. Chim. Acta, 78 (1983) 161.
[95] G.Trotscher, W. Micklitz, H. Schollhorn, U. Thewalt and B. Lippert, Inorg. Chem., 29 (1990) 2541.
[96] W. Micklitz, J. Riede, B. Huber, G. Muller and B. Lippert, Inorg. Chem., 27 (1988) 1979.
[97] H. Schollhorn, U. Thewalt and B. Lippert, Inorg. Chim. Acta, 108 (1985) 77.
[98] R. Faggiani, B. Lippert, C.J.L. Lock and R.A. Speranzini, J. Am. Chem. Soc., 103 (1981) 1111.
[99] D. Neugebauer and B. Lippert, Inorg. Chim. Acta, 67 (1982) 151.
[100] C.J.L. Lock, H.J. Peresie, B. Rosenberg and G. Turner, J. Am. Chem. Soc., 100 (1978) 3371.
[101] R. Faggiani, C.J.L. Lock, R.J. Pollock, B. Rosenberg and G. Turner, Inorg. Chem., 20 (1981) 804.
[102] G. Trovò, G. Bandoli, U. Casellato, B. Corain, M. Nicolini and B. Longato, Inorg. Chem., 29 (1990) 4616.
[103] M. Krumm, I. Mutikainen and B. Lippert, Inorg. Chem., 30 (1991) 884.
[104] M. Krumm, B. Lippert, L. Randaccio and E. Zangrando, J. Am. Chem. Soc., 113 (1991) 5129.
[105] M. Krumm, E. Zangrando, L. Randaccio, S. Menzer and B. Lippert, Inorg. Chem., 32 (1993) 700.
[106] Abstracts from ESF Workshop: Metal Ion Interactions with Nucleic Acids and their Constituents, University of Dortmund, 1993.
[107] M. Krumm, E. Zangrando, L. Randaccio, S. Menzer, A. Danzmann, D. Holthenrich and B. Lippert, Inorg. Chem., 32 (1993) 2183.
[108] (a) J. Fornier, F. Martinez, R. Navarro, A. Redondo, M. Tomas and A.J. Welch, J. Organomet. Chem., 316 (1986) 351; (b) T. Suzuki, N. Iitaka, S. Kurachi, M. Kita, K. Kashiwavara, S. Ohba and J. Fujita, Bull. Chem. Soc. Jpn., 65 (1992) 1817.
[109] I. Sóvágó, A. Kiss and B. Lippert, J. Chem. Soc. Dalton Trans., (1995) 489.
[110] L. Prizant, R. Rivest and A.L. Beauchamp, Can. J. Chem., 59 (1981) 2290.

[111] A.F.M.J. van der Ploeg, G. van Koten, K. Vrieze, A.L. Speck and A.J.M. Duisenberg, Organometallics, 1 (1982) 1066.
[112] (a) F.A. Cotton and R.A. Walton, Struct. Bonding, Berlin, 62 (1985) 1; (b) J.D. Wollin and P.F. Kelly, Coord. Chem. Rev., 65 (1985) 115. (c) T.V. O'Halloran and S.J. Lippard, Isr. J. Chem., 25 (1985) 130.
[113] (a) B. Lippert, J. Clin. Hematol. Oncol., 7 (1977) 26; (b) S.J. Lippard, Science, 218 (1982) 1075.
[114] F.A. Cotton and R.A. Walton, in Multiple Bonds between Metal Atoms, 2nd edn., Claredon Press, Oxford, 1993.
[115] B. Lippert, H. Schollhorn and U. Thewalt, J. Am. Chem. Soc., 108 (1986) 525.
[116] H. Schollhorn, U. Thewalt and B. Lippert, J. Chem. Soc. Chem. Commun., (1986) 258.
[117] B. Lippert, H. Schollhorn and U. Thewalt, Inorg. Chem., 25 (1986) 407.
[118] O. Renn, A. Albinati and B. Lippert, Angew. Chem. Int. Ed. Engl., 29 (1990) 84.
[119] (a) P.K. Mascharak, I. D. Williams and S.J. Lippard, J. Am. Chem. Soc., 106 (1984) 6428; (b) T.V. O'Halloran, P.K. Mascharak, I.D. Williams, M.M. Roberts and S.J. Lippard, Inorg. Chem., 26 (1987) 1261.
[120] B. Lippert, H. Schollhorn and U. Thewalt, Z. Naturforsch. Teil B, 38 (1983)1441.
[121] H. Schollhorn, P. Eisenmann, U. Thewalt and B. Lippert, Inorg. Chem., 25 (1986) 3384.
[122] D.M.L. Goodgame, R.W. Rollins, A.M.Z. Slawin, D.J.Williams and P.W. Zard, Inorg. Chim. Acta, 120 (1986) 91.
[123] D.M.L. Goodgame, R.W. Rollins and A.C. Skapski, Inorg. Chim. Acta, 83 (1984) L11.
[124] D.M.L. Goodgame, A.M.Z. Slawin, D.J.Williams and P.W. Zard, Inorg. Chim. Acta, 148 (1988) 5.
[125] K.Umakoshi and Y.Sasaki, Quadruply bridged dinuclear complexes of platinum, palladium and nickel, in Advances in Inorganic Chemistry, Vol. 40, 1994, p. 187.
[126] I. Mutikainen, O. Orama, A. Pajunen and B. Lippert, Inorg. Chim. Acta, 137 (1987) 189.
[127] G. Frommer, F. Lianza, A. Albinati and B. Lippert, Inorg. Chem., 31 (1992) 2434.
[128] B. Lippert and U.Schubert, Inorg. Chim. Acta, 56 (1981) 15.
[129] (a) W. Micklitz, G. Muller, J. Riede, and B. Lippert, J. Chem. Soc. Chem. Commun., (1987) 76; (b) W. Micklitz, G. Muller, B. Huber, J. Riede, F. Rashwan, J. Heinze and B. Lippert, J. Am. Chem. Soc., 110 (1988) 7084.
[130] W. Micklitz, G.Muller, J. Riede and B. Lippert, J. Chem. Soc. Chem. Commun., (1987) 76.
[131] O. Renn, B. Lippert and I. Mutikainen, Inorg. Chim. Acta, 208 (1993) 219.
[132] B. Lippert and D. Neugebauer, Inorg. Chim. Acta, 46 (1980) 171.
[133] A. Schreiber, O. Krizanovic, E.C. Fusch, B. Lippert, F. Lianza, A. Albinati, S. Hill, D.M.L. Goodgame, H. Stratemeier and M.A. Hitchman, Inorg. Chem., 33 (1994) 6101.
[134] C. Mealli, F. Pichierri, L. Randaccio, E. Zangrando, M. Krumm, D. Holthenrich and B. Lippert, Inorg. Chem., 34 (1995) 3418.
[135] (a) R. Hoffmann and W.N. Lipscomb, J. Chem. Phys., 36 (1962) 2179; (b) R. Hoffman and W.N. Lipscomb, J. Chem. Phys., 37 (1962) 3489; (c) R.J. Hoffmann, J. Chem. Phys., 39 (1963) 1397; (d) J.Ammeter, H.B. Burgi, J.C. Thibeault and R.J.Hoffmann, J. Am. Chem. Soc., 100 (1978) 3686; (e) C. Mealli and D.M. Proserpio, J. Chem. Ed., 67 (1990) 399.
[136] T.A. Albright, J.K. Burdett and M.W. Whangbo, Orbital Interactions in Chemistry, Wiley, New York, 1985.
[137] G.G. Christoph and Y.B. Koh, J. Am. Chem. Soc., 101 (1979) 1422.
[138] R.E. Rundle, J. Phys. Chem., 61 (1957) 45.
[139] C.G. Arena, G. Ciani, D. Drommi, F. Faraone, D.M. Proserpio and E. Rotondo, J. Organomet. Chem., 484 (1994) 71.
[140] M. Goodgame and D.A. Jakubovic, Coord. Chem. Rev., 79 (1987) 97.
[141] B. Lippert, Inorg. Chim. Acta, 55 (1981) 5.
[142] B. Lippert and D. Neugebauer, Inorg. Chem., 21 (1982) 451.
[143] B. Lippert, H. Schollhorn and U. Thewalt, Inorg. Chem., 26 (1987) 1736.
[144] U. Thewalt, D. Neugebauer and B. Lippert, Inorg. Chem., 23, (1984) 1713.
[145] H. Schollhorn, U. Thewalt and B. Lippert, J. Chem. Soc. Chem. Commun., (1984) 769.
[146] D. Holthenrich, M. Krumm, E. Zangrando, F. Pichierri, L. Randaccio and B.Lippert, J. Chem. Soc. Dalton Trans., (1995) 3275.

[147] G. Raudaschl-Sieber, H. Schollhorn, U. Thewalt and B. Lippert, J. Am. Chem. Soc., 107 (1985) 3591.
[148] S. Jaworski, S. Menzer, B. Lippert and M. Sabat, Inorg. Chim. Acta, 205 (1993) 31.
[149] L. Schenetti, G. Bandoli, A. Dolmella, G. Trovò and B. Longato, Inorg. Chem., 33 (1994) 3169.
[150] L. Labib, M.El-Essawi, W. Massa and J. Loberth, Angew. Chem., 100 (1988) 1194.
[151] H. Rauter, E.C. Hillgeris and B.Lippert, J. Chem. Soc. Chem. Commun., (1992) 1385.
[152] R. El-Mehdawi, F.R. Fronczek and D.M. Roundhill, Inorg. Chem., 25 (1986) 3714.
[153] CSD System Documentation, Vols. 1–4, Cambridge, UK, October 1992.